

## Electron correlation, metallization, and Fermi-level pinning at ultrathin K/Si(111) interfaces

H. H. Weitering\* and J. Chen

*Department of Physics, University of Pennsylvania, Philadelphia, Pennsylvania 19104*

N. J. DiNardo

*Department of Physics and Atmospheric Science, Drexel University, Philadelphia, Pennsylvania 19104*

E. W. Plummer

*Department of Physics and Astronomy, University of Tennessee, Knoxville, Tennessee 37996  
and Solid State Division, Oak Ridge National Laboratory, Oak Ridge, Tennessee 37831*

(Received 31 March 1993)

In this paper we present a detailed photoemission study of the K/Si(111)7×7 and K/Si(111)( $\sqrt{3}\times\sqrt{3}$ )R30°-B interfaces. Angle-resolved valence-band spectroscopy reveals the presence of an almost dispersionless interface state below  $E_F$ . Both interfaces are clearly nonmetallic at room-temperature saturation coverage. We critically address the issues of charge transfer and Fermi-level pinning by a detailed analysis of the K 3*p* and Si 2*p* core-level spectra. We conclude that, up to saturation coverage, correlation effects determine the electronic properties of these interfaces. Metallization occurs during the development of the second layer at cryogenic temperatures.

### I. INTRODUCTION

Alkali-metal adsorbates on clean semiconductor surfaces are considered ideal model systems for fundamental studies of interfacial metallization and Schottky barrier formation. It may seem surprising that the classic Langmuir-Taylor model<sup>1</sup> for alkali-metal adsorption still has significant impact on today's understanding of the alkali-metal-semiconductor interface. In this model, the alkali-metal transfers its valence electron to the substrate forming a large surface dipole, resulting in a dramatic decrease of the work function. At higher coverage, the alkali-metal atoms begin to interact and a depolarization mechanism takes over, resulting in the metallization of the overlayer and the partial restoration of the work function.

Intensive research efforts over the past few decades have not only brought new insights into alkali-metal/semiconductor systems, but also many controversies. Basic issues such as interface structure, the nature of the chemical bond, and interfacial metallization are still subject to scientific discussions. For example, numerous papers have already dealt with the atomic structure of the K/Si(100)2×1 interface.<sup>2</sup> Yet, no consensus has been reached. Similarly, the electronic properties of this interface are still ambiguous. Whereas valence-band photoemission studies have suggested that this interface is nonmetallic at room-temperature (RT) saturation coverage,<sup>3</sup> inverse photoemission<sup>4</sup> and scanning-tunneling-microscopy (STM) studies suggest otherwise.<sup>5,6</sup> Even more confusing, K 3*p* core-level photoemission<sup>7</sup> and laser-induced second-harmonic-generation<sup>8</sup> experiments suggest a sudden onset of metallization far below RT saturation coverage. Similar discrepancies between valence-band and core-level photoemission studies have been reported for the

Cs/GaAs(110) interface.<sup>9–11</sup> One might argue that valence-band photoemission lacks the sensitivity for detecting alkali-metal-induced interface states near  $E_F$  at low coverages. However, electron-energy-loss studies on the Cs/GaAs(110) interface corroborate the valence-band photoemission studies.<sup>12</sup>

Some of the experimental discrepancies may possibly be due to experimental difficulties in obtaining atomically clean alkali-metal overlayers. For example, Soukiassian *et al.* recently showed that the absolute alkali-metal coverage is very sensitive to small amounts of hydrogen and oxygen.<sup>5</sup> Another complicating factor is that the absolute saturation coverage may in fact be strongly temperature dependent near RT.<sup>13</sup> This not only implies that a comparison between different RT studies may be nebulous, but also that the interface may be quite disordered since the adatom mobilities are high, complicating STM studies due to, e.g., tip-induced surface modification.<sup>5,14</sup>

Intuitively, a theoretical description of the alkali-metal/semiconductor interface may seem quite straightforward because of the jelliumlike properties of the alkali metals. However, even the fundamental issue of the nature of the chemical bond between the alkali-metal atom and substrate atoms has not been settled. For example, calculations of Batra for Si(100) and Si(111) suggest that alkali-metal atoms form predominantly ionic bonds with the semiconductor surface atoms, even near saturation coverage.<sup>15</sup> No overlayer bands can be identified near  $E_F$  meaning that the overlayer must be insulating and that interfacial metallization occurs in the outermost atomic layers of the substrate (substrate metallization). However, other calculations have shown a varying degree of ionicity.<sup>16,17</sup>

Recently, it has been recognized that a full understanding of the phenomenon of metallization not only requires a thorough understanding of the nature of the chemical

bond between the alkali-metal atom and the substrate but that one also needs to address the issue of electron localization. Because the overlap between neighboring adatom states or dangling-bond-type surface states may be small, it is perfectly conceivable that many semiconductor surfaces and ultrathin metal-semiconductor interfaces may represent two-dimensional Mott insulators.<sup>12,18-25</sup> Obviously, the structure and density of overlayer atoms are crucial parameters. Unfortunately, the absolute coverage is often unknown, leading to structural models that are based on electron-counting arguments, assuming that a semiconducting interface requires an even number of valence electrons per surface unit cell.<sup>26,27</sup> The potential fallacy of this reasoning becomes clear when electron-electron correlation effects must be taken into account.<sup>28</sup> Therefore, a mechanism of interfacial metallization can only be resolved if both the structure and absolute coverage are known.

In this paper, we present a detailed angle-resolved photoemission study on the K/Si(111)7×7 and K/Si(111)(√3×√3)R30°-B interfaces [the latter interface consists of a K overlayer on a Si(111) surface with a boron underlayer; see Fig. 1]. Although absolute coverages for these interfaces have yet to be determined, a comparative study of these structurally similar interfaces

reveals some important aspects of interfacial bonding and metallization<sup>29,30</sup> since the electronic properties of the clean Si(111)7×7 and Si(111)(√3×√3)R30°-B surfaces are distinctly different. Whereas the clean Si(111)7×7 surface is metallic,<sup>31,32</sup> the Si(111)(√3×√3)R30°-B surface is semiconducting.<sup>33,34</sup> A unique property of the latter surface is that trivalent B occupies a fivefold-coordinated subsurface site ( $S_5$ ), directly below a Si adatom at the  $T_4$  position<sup>33-36</sup> (Fig. 1). The presence of B stabilizes the (√3×√3)R30° surface reconstruction with respect to the (7×7) reconstruction and strongly modifies the electronic properties of the Si(111) surface. Consequently, the number of valence electrons involved in interfacial bonding must be different for the (7×7) and (√3×√3)R30°-B interfaces. This allows us to address relevant issues such as charge transfer<sup>29,30</sup> and localization.

Based on a recent high-resolution Si 2*p* core-level study, Ma *et al.* concluded that the K-Si bond is predominantly ionic at the K/Si(111)(√3×√3)R30°-B interface<sup>30</sup> while it is covalent at the K/Si(111)7×7 interface.<sup>29</sup> They speculated that this can be qualitatively understood, realizing that occupancy of the K-Si hybrid state is different. Single-particle considerations would then predict that the K/Si(111)(√3×√3)R30°-B interface is metallic for all coverages up to saturation. In this paper, however, we will demonstrate that both interfaces are clearly *nonmetallic*. We will argue that correlation effects are important in determining the electronic properties of these interfaces. Furthermore, we will address the issues of charge transfer and Fermi-level pinning by a detailed analysis of the K 3*p* and Si 2*p* core-level spectra. Finally, we demonstrate that these interfaces become metallic during the growth of a second K layer at cryogenic temperatures.

## II. EXPERIMENT

Angle-resolved photoemission experiments were carried out at beam line U12<sup>b</sup> of the National Synchrotron Light Source at Brookhaven National Laboratory. The incident light was dispersed by a toroidal grating monochromator. The total energy resolution of our photoemission spectra was 0.15 eV at a photon energy of 20.9 eV, 0.3 eV at 40 eV, and 0.5 eV at 100 eV. The hemispherical electron-energy analyzer has an acceptance angle of ±2°. Lightly doped *n*-type Si(111) wafers ( $\rho=1 \Omega \text{ cm}$ ) were cleaned by the Shiraki method<sup>37</sup> and inserted into the vacuum chamber (base pressure  $7 \times 10^{-11}$  mbar). The thin oxide layer was removed by direct resistive heating to 800 °C. After cooling to room temperature, sharp (7×7) low-energy electron diffraction (LEED) patterns were consistently observed. The Si(111)(√3×√3)R30°-B surface was prepared by exposing the clean (7×7) surface to decaborane ( $B_{10}H_{14}$ ) and by subsequent annealing at 900 °C. Following the procedure of Lyo, Kaxiras, and Avouris,<sup>33</sup> After cooling to RT, a very sharp (√3×√3)R30° LEED pattern with a remarkably low background intensity was observed, indicating near-perfect ordering.

K was deposited at RT onto the clean (7×7) or

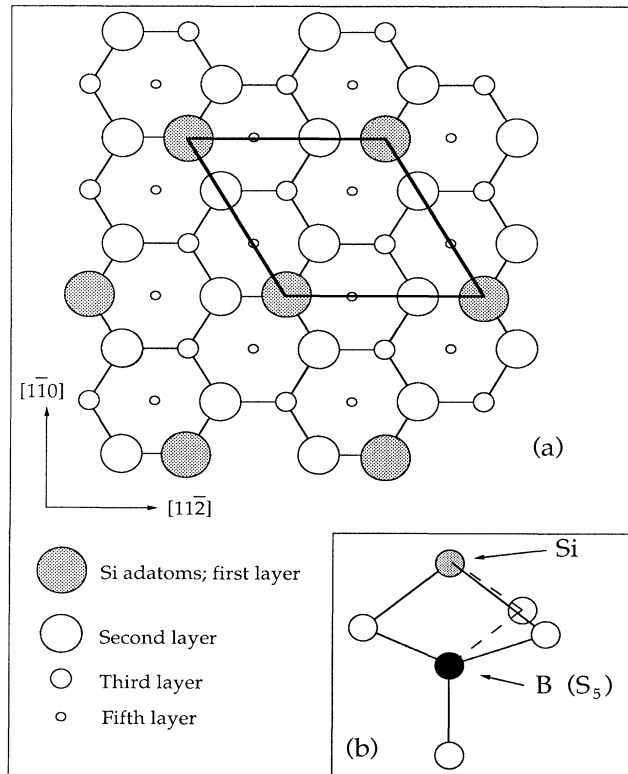


FIG. 1. Atomic structure of the Si(111)(√3×√3)R30°-B surface (a). The shaded circles represent the Si adatoms which are located directly above the fivefold-coordinated B atoms, as depicted in (b). The Si adatom sites are the most likely chemisorption sites for K atoms.

$(\sqrt{3}\times\sqrt{3})$  surfaces, using thoroughly degassed SAES dispensers, located close to the sample ( $\sim 2.5$  cm). In order to accelerate the outgassing procedure, the source current was increased to 7 A for about 5 min regularly. During the deposition experiments, the source current was kept at 5.5 A. Under these conditions, the pressure increase  $\Delta p$  during deposition never exceeded  $2\times 10^{-11}$  mbar.

Upon K deposition, the  $(7\times 7)$  and  $(\sqrt{3}\times\sqrt{3})$  LEED patterns were preserved, although the background intensity was slightly enhanced. The relative K coverage ( $\Theta/\Theta_{\text{sat}}$ ) was determined by measuring the K  $3p$  core-level intensity as a function of deposition time for both interfaces. The work function was determined from the secondary cutoff in the photoelectron spectrum. Coverage-dependent measurements were always performed on a freshly prepared interface, i.e., after each measurement, the K layer was desorbed. This way we avoided accumulation of contaminants (mainly oxygen and hydrogen from the getter source), which is known to affect the growth mode and absolute coverage.<sup>5,6</sup> During angle-dependent measurements, the K layer was renewed at least once every 40 min. After depositing another layer, the previous measurement was repeated in order to ensure that the data were not affected by contamination.

### III. VALENCE-BAND PHOTOEMISSION

Angle-resolved ultraviolet photoemission spectroscopy (UPS) data were obtained from the clean Si(111) $(\sqrt{3}\times\sqrt{3})R30^\circ$ -B surface, the K/Si(111) $7\times 7$  interface and the K/Si(111) $(\sqrt{3}\times\sqrt{3})R30^\circ$ -B interface. For spectra from the clean Si(111) $7\times 7$  surface, we refer to Hansson and Uhrberg.<sup>38</sup>

The initial-state energy  $E_i$  is defined with respect to the Fermi level, as determined from the Fermi edge of a thick K layer grown at 77 K. The angle of incidence  $\alpha_i$  is defined with respect to the surface normal. Electron distribution curves (EDC's) were recorded with the parallel wave vector  $k_{\parallel}$  along the  $[\bar{1}\bar{1}0]$  azimuth of the Si lattice, corresponding to the  $\bar{\Gamma}\bar{K}$  direction of the  $(1\times 1)$  surface Brillouin zone (SBZ) (Fig. 2). Because the azimuthal orientation of the sample could not be varied, we chose to align the sample with its  $[1\bar{1}0]$  azimuth in the polarization plane of the light ( $p$  polarization).

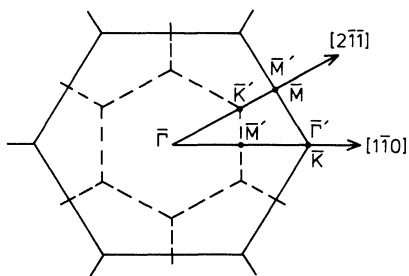


FIG. 2. The  $(1\times 1)$  and  $(\sqrt{3}\times\sqrt{3})$  surface Brillouin zones of the Si(111) surface (solid and dashed lines, respectively).

#### A. Coverage-dependent UPS at room temperature

Upon K deposition at RT, the work function of the  $(7\times 7)$  and  $(\sqrt{3}\times\sqrt{3})$  interfaces strongly decreases as a function of deposition time (Fig. 3). After 200 s of deposition time, both the work function and the K  $3p$  core-level intensity remain constant ( $\Delta\Phi \approx -2.9$  eV). We conclude that a saturated monolayer is formed after 200 s of RT deposition. Interestingly, unlike the K/Si(100) $2\times 1$  interface,<sup>13</sup> the work function does not pass through a minimum.

Normal emission valence-band photoelectron spectra were recorded for the K/Si(111) $7\times 7$  and K/Si(111) $(\sqrt{3}\times\sqrt{3})R30^\circ$ -B interfaces as a function of coverage (Fig. 4). The corresponding values of  $\Delta\Phi$  are indicated for each spectrum. The spectrum of the clean  $(7\times 7)$  surface reveals the presence of the well-known adatom state  $S_1$  at  $E_F$  and the rest-atom state  $S_2$  at 0.8 eV below  $E_F$ .<sup>38</sup>  $S_1$  is usually considered responsible for the metallic nature of the clean Si(111) $7\times 7$  surface.<sup>38,39</sup>

Upon K deposition, the  $S_1$  and  $S_2$  surface states shift to higher binding energy and eventually appear to merge

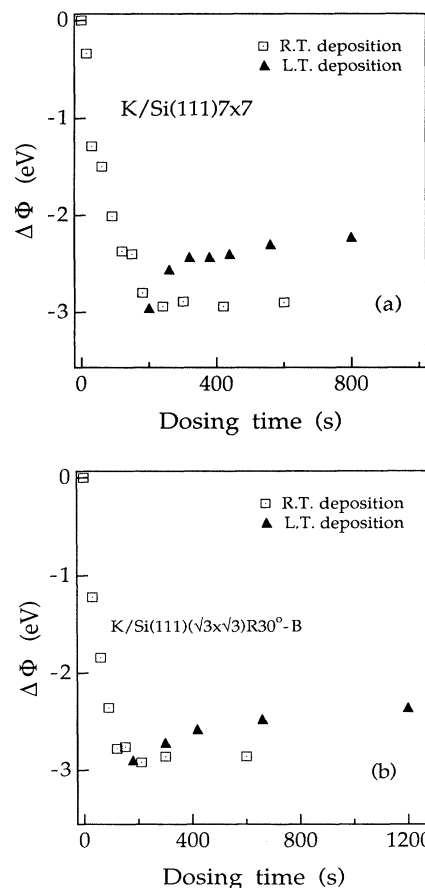


FIG. 3. Work function decrease for the K/Si(111) $7\times 7$  interface (a) and the K/Si(111) $(\sqrt{3}\times\sqrt{3})R30^\circ$ -B interface (b), as measured from the secondary cutoff in the photoemission spectrum. The low-temperature data are discussed in Sec. VI.

into a different interface state ( $A_1$ ). At an intermediate coverage, corresponding to  $\Delta\Phi \approx -2.0$  eV, the photoemission intensity at  $E_F$  has disappeared. At saturation coverage ( $t \gtrsim 200$  s,  $\Delta\Phi \approx -2.9$  eV), the interface is clearly nonmetallic. This is consistent with the fact that the work function does not pass through a minimum up to saturation coverage (Fig. 3).<sup>40</sup> These observations generally agree with a previous angle-integrated photoemission study by Magnusson and Reihl.<sup>41</sup>

In contrast to the clean ( $7 \times 7$ ) surface, no surface states were observed in the normal emission valence-band spectrum of the clean ( $\sqrt{3} \times \sqrt{3}$ ) surface [Fig. 4(b)]. The Fermi level is situated 0.1 eV above the valence-band maximum (VBM), as discussed in Sec. IV. Upon K deposition, an interface state shows up just below the Fermi energy ( $B_1$ ). This state does not cross  $E_F$  although it comes very close. No semiconductor-to-metal transition can be observed up to saturation coverage. This is con-

sistent with the absence of a work function minimum for this system.<sup>40</sup>

### B. Angle-dependent UPS at room temperature

In Fig. 5, photoemission spectra of the saturated K/Si(111) $7 \times 7$  (a) and K/Si(111)( $\sqrt{3} \times \sqrt{3}$ )R30°-B (b) interfaces are plotted for different emission angles along the  $[1\bar{1}0]$  azimuth. These spectra reveal the presence of a K-induced surface state just below the Fermi energy, which is labeled  $A_1$  or  $B_1$  for the saturated K/Si(111) $7 \times 7$  or K/Si(111)( $\sqrt{3} \times \sqrt{3}$ )R30°-B interface, respectively. The two-dimensional dispersion of these states is very small, indicating localized behavior. At the ( $7 \times 7$ ) interface,  $A_1$  disperses from 0.9 eV below  $E_F$  at the center of the ( $1 \times 1$ ) SBZ ( $\bar{\Gamma}$ ) to 1.25 eV below  $E_F$  at  $\bar{K}$ . Thus the bandwidth is  $\approx 0.35$  eV. At the ( $\sqrt{3} \times \sqrt{3}$ ) interface,  $B_1$  disperses from 0.65 eV below  $E_F$  at  $\bar{\Gamma}$  to 0.85 eV below  $E_F$  at  $\bar{K}$ . The bandwidth of  $B_1$  is very

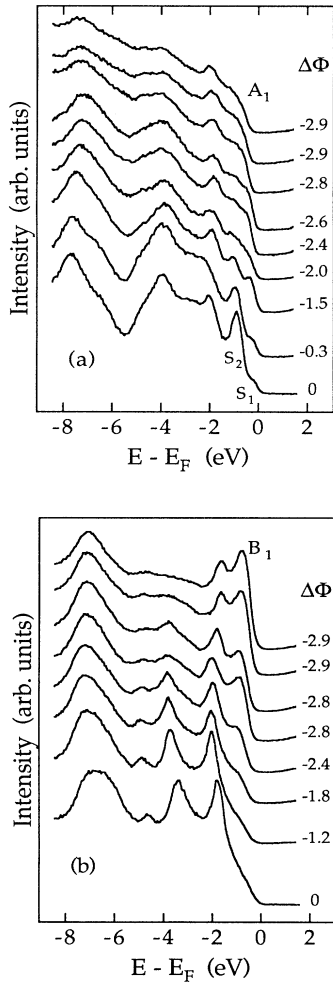


FIG. 4. Normal emission spectra of the K/Si(111) $7 \times 7$  (a) and K/Si(111)( $\sqrt{3} \times \sqrt{3}$ )R30°-B (b) interfaces as a function of K coverage at RT. The incidence angle  $\alpha_i$  for the polarized light is 45°. The photon energy is 20.9 eV.

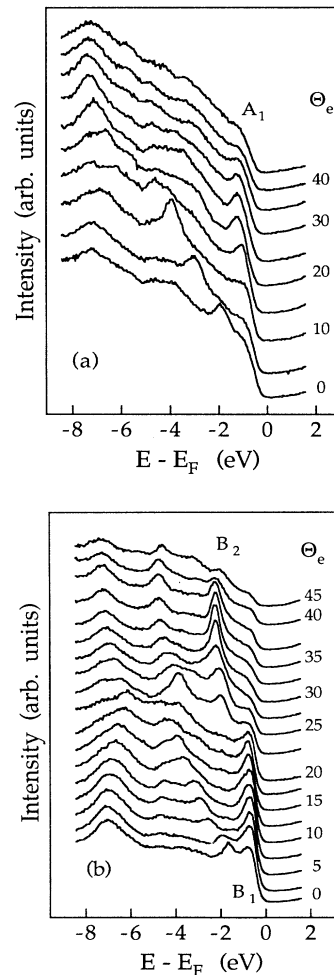


FIG. 5. Angle-dependent photoemission spectra along  $[1\bar{1}0]$  for the RT saturated K/Si(111) $7 \times 7$  (a) and the K/Si(111)( $\sqrt{3} \times \sqrt{3}$ )R30°-B (b) interfaces. The incident angle  $\alpha_i$  for the polarized light is 45°. The photon energy is 20.9 eV.

small (0.2 eV). No Fermi-level crossing can be observed for all emission angles measured. This has been verified at different photon energies.

In order to reveal the nature of the K-induced surface states, we studied the surface-state emission at the  $(\sqrt{3}\times\sqrt{3})$  interface under various excitation conditions. From Fig. 6 it becomes clear that  $B_1$  is enhanced by increasing the angle of incidence  $\alpha_i$  or, equivalently, by increasing the normal component of the polarization vector. This indicates that  $B_1$  must have substantial dangling-bond character. Since the polarization vector is in the emission plane, we also conclude that the surface-state wave function must have even symmetry with respect to the emission plane. Most likely, this surface state comprises a mixture of the Si dangling bonds and K 4s orbitals, retaining substantial dangling-bond character.

At the  $(\sqrt{3}\times\sqrt{3})$  interface, we also observe another surface state ( $B_2$ ) at approximately 2.2 eV below the Fermi level [ $\Theta_e > 20^\circ$ ; Fig. 5(b)]. The dispersion of this surface state is symmetric around  $\Theta_e = 33^\circ$ , which corresponds to the  $\bar{K}$  point of the  $(1\times 1)$  SBZ or the  $\bar{\Gamma}$  point of the second  $(\sqrt{3}\times\sqrt{3})$  SBZ (Fig. 2). This behavior resembles that of the well-known backbond surface state at the Si(111) $(\sqrt{3}\times\sqrt{3})$ R30°-B,<sup>42,34</sup> Si(111) $(\sqrt{3}\times\sqrt{3})$ R30°-Al,<sup>43-44</sup> Si(111) $(\sqrt{3}\times\sqrt{3})$ R30°-Ga,<sup>45</sup> and Si(111) $(\sqrt{3}\times\sqrt{3})$ R30°-In (Ref. 46) surfaces. This backbond state is mainly composed of the in-plane  $p_x, p_y$  orbitals of the adatoms in the  $(\sqrt{3}\times\sqrt{3})$  surface reconstruction and the dangling bonds of the Si substrate.<sup>47</sup> For comparison, we have plotted the angle-dependent spectra of the clean Si(111) $(\sqrt{3}\times\sqrt{3})$ R30°-B

surface in Fig. 7. In this figure, the backbond surface state is labeled  $B_2'$ . The similarity between the spectra from the clean Si(111) $(\sqrt{3}\times\sqrt{3})$ R30°-B surface (Fig. 7) and RT saturated K/Si(111) $(\sqrt{3}\times\sqrt{3})$ R30°-B interface [Fig. 5(b)] is clear and strongly suggests that  $B_2$  in Fig. 5(b) can be identified as a backbond surface state. In order to confirm this assignment, we have recorded valence-band spectra for  $\Theta_e = 33^\circ$  as a function of K coverage (Fig. 8). The bottom spectrum in Fig. 8 corresponds to the clean Si(111) $(\sqrt{3}\times\sqrt{3})$ R30°-B surface. Upon K deposition, the backbond state ( $B_2'$ ) rapidly shifts to higher binding energy. The important conclusion is that the backbond surface state is not disrupted by K adsorption, which proves that the Si-adatom geometry of the Si(111) $(\sqrt{3}\times\sqrt{3})$ R30°-B surface remains unaltered, i.e., no Si-Si bonds are broken. The K-induced shift of the backbond surface state is opposite to the K-induced band bending shift (Sec. IV) and must therefore be attributed to the K-Si interaction.

The spectra from the clean Si(111) $(\sqrt{3}\times\sqrt{3})$ R30°-B surface and the RT saturated K/Si(111) $(\sqrt{3}\times\sqrt{3})$ R30°-B interface have been converted into a dispersion plot (Fig. 9), using standard procedures.<sup>48</sup> In this plot, the binding energies are referred to the VBM ( $E_F - E_{\text{VBM}}$ ) is determined by Si 2p core-level spectroscopy; Sec. IV). The projected band structure was taken from Ivanov, Mazur, and Pollmann.<sup>49</sup> The K-induced surface states appear below the VBM and are located in the projected band gap of Si. It is interesting to note that K adsorption not only causes a downward shift of the backbond surface state by roughly 0.3 eV but also reduces its dispersion.

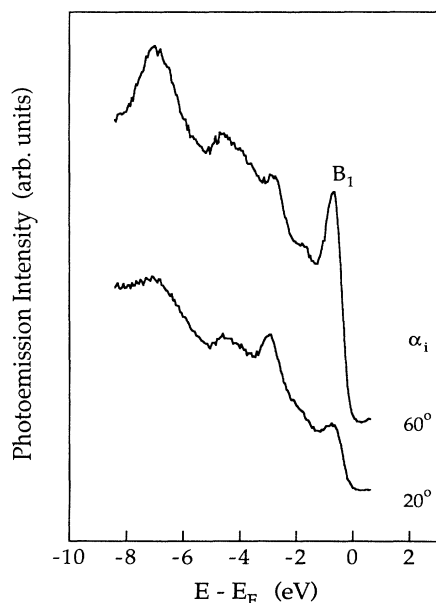


FIG. 6. Incident-angle ( $\alpha_i$ ) dependence of the surface-state emission ( $B_1$ ) at the K/Si(111) $(\sqrt{3}\times\sqrt{3})$ R30°-B interface near the center of the  $(1\times 1)$  SBZ. The photon energy is 20.9 eV. The emission angle  $\Theta_e = 5^\circ$ .

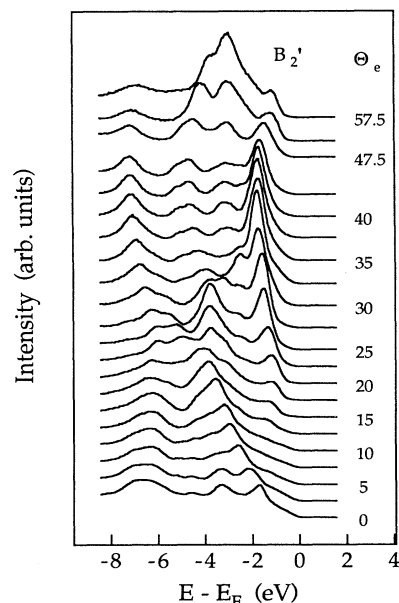


FIG. 7. Angle-dependent photoemission spectra along  $[1\bar{1}0]$  of the clean Si(111) $(\sqrt{3}\times\sqrt{3})$ R30°-B surface. The incident angle  $\alpha_i$  for the polarized light is  $45^\circ$ . The photon energy is 20.9 eV.  $B_2'$  is the backbond surface state.

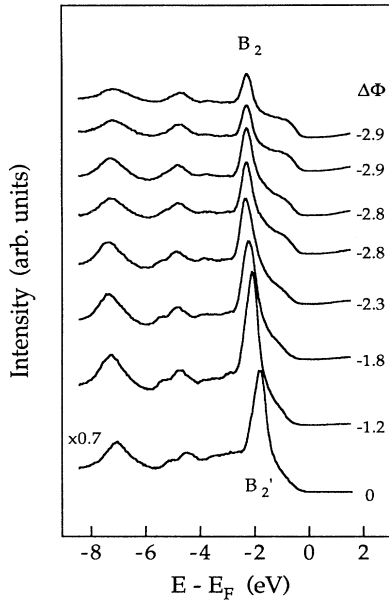


FIG. 8. Coverage dependence of the valence-band spectrum near  $\bar{K}(\bar{\Gamma}')$  for the  $\text{K}/\text{Si}(111)(\sqrt{3} \times \sqrt{3})R 30^\circ\text{-B}$  interface. The incident angle  $\alpha_i$  for the polarized light is  $45^\circ$ . The photon energy is 20.9 eV. The backbond surface state for the clean  $\text{Si}(111)(\sqrt{3} \times \sqrt{3})R 30^\circ\text{-B}$  surface is marked as  $B_2'$ . Upon K deposition,  $B_2'$  shifts toward high binding energy. At the room-temperature saturated  $\text{K}/\text{Si}(111)(\sqrt{3} \times \sqrt{3})R 30^\circ\text{-B}$  interface, this state is denoted as  $B_2$ .

### C. Discussion

#### 1. $\text{K}/\text{Si}(111)(\sqrt{3} \times \sqrt{3})R 30^\circ\text{-B}$

Although the atomic structure of the  $\text{K}/\text{Si}(111)(\sqrt{3} \times \sqrt{3})R 30^\circ\text{-B}$  interface has not been determined directly, the persistence of the  $(\sqrt{3} \times \sqrt{3})$  LEED patterns after deposition of K indicates that a K-induced structural rearrangement of the outermost layer of Si atoms is unlikely. Moreover, the persistence of the backbond surface state at the  $(\sqrt{3} \times \sqrt{3})$  interface indicates that the Si adatom geometry remains unaffected. Hence, it is very likely that the K atoms bond directly to the dangling-bond orbitals of the Si adatoms in the  $(\sqrt{3} \times \sqrt{3})$  reconstruction. Since there is only one Si adatom per  $(\sqrt{3} \times \sqrt{3})$  unit cell, the saturation coverage for the  $\text{K}/\text{Si}(111)(\sqrt{3} \times \sqrt{3})R 30^\circ\text{-B}$  interface must be exactly  $\frac{1}{3}$  monolayer (ML). In the following, we will assume an absolute saturation coverage of  $\frac{1}{3}$  ML.

The dangling bonds of the Si adatoms in the clean  $\text{Si}(111)(\sqrt{3} \times \sqrt{3})R 30^\circ\text{-B}$  surface reconstruction are completely empty, due to the presence of trivalent B directly beneath the Si adatom.<sup>34</sup> At saturation coverage, the number of K atoms equals the number of Si adatoms. Since K contributes only one valence electron, there must be one unpaired valence electron per  $(\sqrt{3} \times \sqrt{3})$  unit cell. Consequently, according to band theory, the saturated  $\text{K}/\text{Si}(111)(\sqrt{3} \times \sqrt{3})R 30^\circ\text{-B}$  interface is metallic. However, our photoemission data clearly reveal that this in-

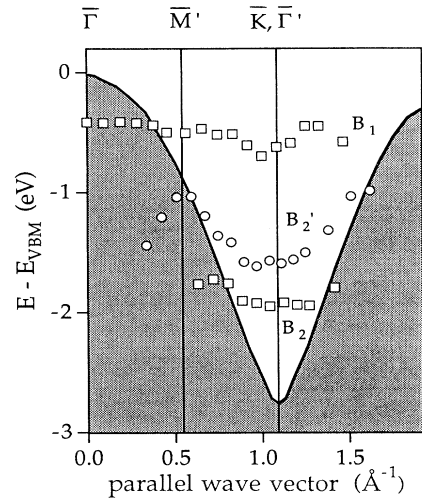


FIG. 9. Diagram showing the energy-vs-wave vector relation for the surface states at the clean  $\text{Si}(111)(\sqrt{3} \times \sqrt{3})R 30^\circ\text{-B}$  surface (circles) and  $\text{K}/\text{Si}(111)(\sqrt{3} \times \sqrt{3})R 30^\circ\text{-B}$  interface (squares). The shaded area is the projection of the bulk Si bands onto the (111) surface (Ref. 49).

terface is nonmetallic. The uppermost surface state ( $B_1$ ) is located at 0.65 eV below the Fermi level near the zone center and slightly disperses downward for wave vectors approaching the zone boundaries. One could argue that photoemission lacks the sensitivity to detect alkali-metal-induced surface states near  $E_F$  if they have a predominantly  $s$  character. However, it is very likely that the alkali-metal wave function hybridizes with the Si dangling bonds, resulting in a bonding state in the lower part of the band gap and an antibonding state forming a resonance with the conduction-band continuum (Fig. 10).<sup>12, 18, 30, 50</sup> Hence,  $B_1$  probably represents the bonding combination of K  $4s$  orbitals and Si dangling bonds. According to band theory, this bonding surface state should cross  $E_F$  unless there is an even number of valence electrons per  $(\sqrt{3} \times \sqrt{3})$  unit cell, in which case the surface state must be located entirely below  $E_F$  (Fig. 10). This, however, requires precisely two K atoms per Si dangling bond which is unlikely. Therefore, we conclude that band theory cannot explain our observations.

An interesting alternative explanation is that the  $\text{K}/\text{Si}(111)(\sqrt{3} \times \sqrt{3})R 30^\circ\text{-B}$  interface constitutes a two-dimensional Mott-Hubbard insulator. In fact, it has been suggested before that the dangling bonds at the ideally truncated  $\text{Si}(111)$  surface should represent a two-dimensional Mott-Hubbard system because the orbital overlap between neighboring dangling bonds is very small.<sup>21-24</sup> Consequently, the hopping integral  $t$  (also called "overlap energy") is likely to be much smaller than the on-site electron-electron Coulomb repulsion,  $U$ , even though  $U$  is largely screened by the substrate. For example, Harrison has calculated a bare Coulomb repulsion  $U$  for a Si dangling hybrid of 7.6 eV which reduces to a value  $U^* \approx 2.4$  eV after accounting for the polarization of the substrate.<sup>23</sup> Hybridization can result in an even

smaller  $U_{\text{eff}}$  of approximately 0.5 eV.<sup>51</sup> Since  $t < 0.1$  eV at the Si(111)(1×1) surface,<sup>23,24</sup> we obtain  $U_{\text{eff}} \gg t$ , suggesting that the Si(111)(1×1) surface should be an antiferromagnetic Mott-Hubbard insulator.<sup>23,28</sup> However, no experimental evidence for an insulating antiferromagnetic ground state of this surface has been provided to date. The trivial reason is that an unreconstructed Si(111) surface does not exist. The only experimental evidence for significant electron-electron correlation in Si dangling bonds comes from studies of isolated dangling-bond defects in  $\alpha$ -SiH (Ref. 52) or at the Si-SiO<sub>2</sub> interface.<sup>53</sup> More recently, scanning tunneling spectroscopy experiments revealed that  $U_{\text{eff}} > 0.4$  eV for isolated Si dangling-bond defect states at the Si(111)( $\sqrt{3} \times \sqrt{3}$ )R30°-A1 interface.<sup>54</sup>

Our results suggest that electron-electron correlation is responsible for the insulating behavior of the K/Si(111)( $\sqrt{3} \times \sqrt{3}$ )R30°-B interface. Unlike isolated defect states, the dangling-bond-type surface state at the

K/Si(111)( $\sqrt{3} \times \sqrt{3}$ )R30°-B interface must be fully periodic in two dimensions. Hence, this nonmetallic interface possibly exhibits antiferromagnetic ordering.<sup>28</sup> A metallic ground state can only be realized through direct K-K interaction. However, this interaction is expected to be very small since the distance between the hybrid orbitals in the ( $\sqrt{3} \times \sqrt{3}$ ) structure (6.65 Å) is much larger than the interatomic distance of bulk K (4.53 Å). Correspondingly, the dispersion of the dangling-bond-type surface state should be small, in agreement with our photoemission results. The bandwidth  $W$ , as determined from our angle-dependent photoelectron spectra, is  $\approx 0.2$  eV, indicating that  $t < 0.1$  eV.<sup>55</sup>

According to the Hubbard model,  $B_1$  would represent the energy levels of the hole in the photoemission final state (lower Hubbard band<sup>28</sup>). Likewise, there must be a narrow band above  $E_F$  corresponding to the energy levels of the added electron in the final state of the inverse photoemission process (upper Hubbard band<sup>28</sup>). The splitting between these two bands is  $U_{\text{eff}}$ . Unfortunately, due to the lack of inverse photoemission data, we can only give a lower limit for  $U_{\text{eff}}$ . Since  $B_1$  is situated 0.7 eV below  $E_F$ , we conclude that  $U_{\text{eff}} > 0.7$  eV.

We finally note that a Mott-Hubbard insulating ground state has also been proposed previously for the Cs/GaAs(110),<sup>12</sup> Cs/InSb(110),<sup>25</sup> and Na/Si(111)3×1 interfaces.<sup>56</sup> Very recently, theoretical calculations suggested that  $U_{\text{eff}} \approx 0.56$  eV for the Ga dangling-bond orbitals of the K/GaAs(110) interface.<sup>20</sup>

## 2. K/Si(111)7×7

Our LEED and angle-resolved photoemission spectroscopy (ARPES) data strongly suggest that the absolute saturation coverage of the K/Si(111)( $\sqrt{3} \times \sqrt{3}$ )R30°-B interface must be exactly  $\frac{1}{3}$  ML. For K/Si(111)7×7, it is less obvious what the absolute coverage might be, because the angle-resolved photoemission spectra are rather featureless. Therefore, it is not possible to judge whether the backbond surface state of the Si adatoms in the (7×7) reconstruction has disappeared or whether it is simply obscured. In any case, the persistence of the (7×7) LEED pattern indicates that the stacking fault must still be present at saturation coverage. Let us first assume that the adatom geometry is preserved upon K deposition. In that case, there are two possibilities for site occupation. If the K atoms only bond to the adatom dangling-bond orbitals, the absolute saturation coverage would be  $12/49 = 0.24$  ML. On the other hand, if both the adatoms and the rest atoms are involved, the absolute saturation coverage would be  $18/49 = 0.37$  ML. The latter possibility seems to be consistent with the fact that the uptake of K, as measured from the K 3*p* core-level intensity, is almost identical for the (7×7) and ( $\sqrt{3} \times \sqrt{3}$ ) interfaces. Furthermore, Auger data unambiguously reveal that the absolute saturation coverages of both interfaces are nearly equal.<sup>57,58</sup> Although we do not have direct evidence that the adatom geometry remains preserved upon K deposition, we will assume that the K atoms directly bond to the rest-atom and the adatom dangling bonds of the (7×7) reconstructed surface. In

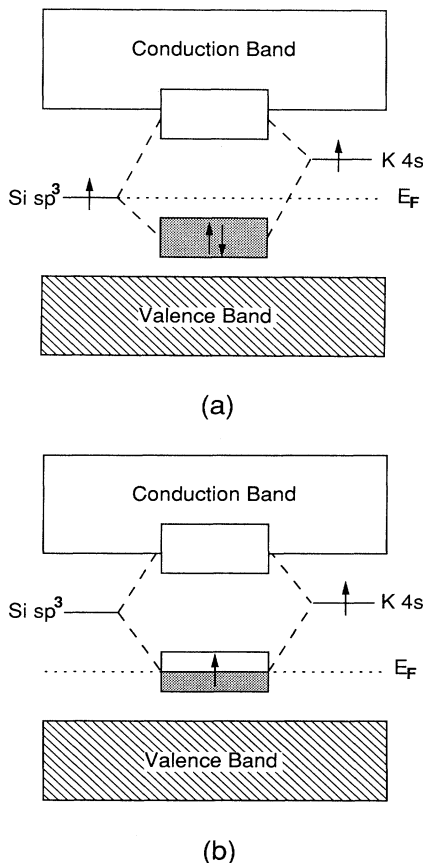


FIG. 10. Schematic diagram of the interfacial band structure for the saturated K/Si(111)7×7 and K/Si(111)( $\sqrt{3} \times \sqrt{3}$ )R30°-B interfaces. According to band theory, the lower surface-state band must be completely filled at the saturated K/Si(111)7×7 interface (a) whereas it is half-filled for the K/Si(111)( $\sqrt{3} \times \sqrt{3}$ )R30°-B interface (b). According to a single-particle picture, the K/Si(111)( $\sqrt{3} \times \sqrt{3}$ )R30°-B interface should be metallic.

that case, the dangling-bond orbitals are completely filled at RT saturation coverage. Indeed, Fig. 5(a) reveals that the K-induced interface state is located below  $E_F$ .

We speculate that the following scenario may qualitatively explain our photoemission data. At the clean ( $7\times 7$ ) surface, the adatom states and rest-atom states interact, resulting in a completely filled surface state at  $\approx 0.8$  eV below  $E_F$  (usually denoted as the rest-atom state) and a partially filled surface state at  $E_F$  (usually denoted as the adatom state).<sup>38</sup> Because the number of adatoms and rest atoms in the ( $7\times 7$ ) reconstruction is different, the adatom state must cross  $E_F$ . Upon K adsorption, these states move downward due to hybridization with the K  $4s$  orbitals. Bonding to the K atoms reduces the energy splitting between the adatom and rest-atom states, thereby increasing their mutual interaction. This accounts for the observation that upon K deposition, the  $S_1$  and  $S_2$  surface states merge into a different interface state,  $A_1$ , which has significant dispersion (0.35 eV). This dispersion is much larger than that of the rest-atom or adatom states of the clean ( $7\times 7$ ) surface ( $\approx 0.15$  and  $\approx 0$  eV, respectively<sup>59</sup>). Magnusson *et al.* proposed a similar scenario for Cs adsorption on Si(111) $7\times 7$ .<sup>60</sup> However, an important difference is that the K/Si(111) $7\times 7$  interface is semiconducting over a wide coverage range, up to RT saturation, while the Cs/Si(111) $7\times 7$  interface metallizes near saturation.<sup>60</sup>

Unlike the situation for the K/Si(111)( $\sqrt{3}\times\sqrt{3}$ )R 30°-B interface, these observations can be understood in a single-particle picture. According to band theory, a crystal with an odd number of valence electrons per unit cell must always be a metal whereas a crystal with an even number of valence electrons per unit cell can either be a metal or a semiconductor, depending on the details of the band structure. The semiconducting nature of the K/Si(111) $7\times 7$  interface can simply be understood in a local bonding picture, as depicted in Fig. 10(a). On the other hand, the metallic nature of the Cs/Si(111) $7\times 7$  interface suggests that at least two different surface-state bands must cross  $E_F$ .<sup>27</sup> Obviously, this cannot be understood in a local bonding picture, suggesting that the metallic nature of this interface is due to direct Cs-Cs interaction. This is reasonable because the in-plane nearest-neighbor distance of the surface dangling bonds (4.43 Å) is much smaller than the interatomic distance of bulk Cs (5.24 Å). This suggests that the metallic nature of the Cs/Si(111) $7\times 7$  interface is most likely due to the formation of an overlayer band crossing  $E_F$ . It must be emphasized that even though the nonmetal to metal transition at the Cs/Si(111) $7\times 7$  interface marks the transition from a localized “bondlike” situation to a delocalized “bandlike” situation, it does not require a many-body explanation.

The energy of the K-induced surface state ( $A_1$ ) at the center of the SBZ is 0.9 eV below  $E_F$  or 0.6 eV below  $E_{\text{VBM}}$ . This should be compared with the energies of the adatom state and rest-atom state at the clean ( $7\times 7$ ) surface, which are located at 0.45 eV above  $E_{\text{VBM}}$  and 0.2 eV below  $E_{\text{VBM}}$ , respectively.<sup>61</sup> According to Magnusson and Reihl, the much higher binding energy of the  $A_1$  sur-

face state is due to electron-electron repulsion in the Si dangling bonds.<sup>41</sup> However, the only many-body effect that could account for the larger photoionization potential is the on-site hole-hole repulsion in the photoemission final state. Since the initial state at the saturated K/Si(111) $7\times 7$  interface represents a closed-shell configuration, there is only one hole in the final state and the observed binding energy should be equal to the ionization energy of the single-particle eigenstate. In contrast, hole-hole correlation in the photoemission final state at the K/Si(111)( $\sqrt{3}\times\sqrt{3}$ )R 30°-B interface increases the final-state energy. Hence, in the photoemission spectrum of this interface,  $B_1$  is shifted away from  $E_F$ , thus representing the lower Hubbard band. It is likely that downward shift of  $A_1$  at the K/Si(111) $7\times 7$  interface is due to hybridization.

Electron-electron correlation effects are probably important for determining the electronic properties of the K/Si(111) $7\times 7$  interface at coverages below saturation. It must be realized that this interface already becomes semiconducting at low coverage and remains semiconducting up to saturation coverage. Obviously, this cannot be understood on the basis of band theory. A reasonable explanation is that, at intermediate coverages, only a fraction of the available dangling-bond orbitals is hybridized with the K  $4s$  orbitals. Hence, the two-dimensional periodicity of the dangling-bond-type surface states is disrupted, leading to charge localization in the remaining half-filled states. This situation resembles that of the half-filled dangling-bond defect states at the Si(111)( $\sqrt{3}\times\sqrt{3}$ )R 30°-A1 interface.<sup>54</sup>

#### IV. Si 2p CORE LEVELS: RESULTS AND DISCUSSION

In order to determine the position of  $E_F$  for the different interfaces, we recorded Si 2p core-level spectra from the clean Si(111) $7\times 7$  and Si(111)( $\sqrt{3}\times\sqrt{3}$ )R 30°-B surfaces and from the RT saturated K/Si(111) $7\times 7$  and K/Si(111)( $\sqrt{3}\times\sqrt{3}$ )R 30°-B interfaces. Since the position of the Fermi level at the clean Si(111) $7\times 7$  surface is known,<sup>61</sup> we can in principle determine  $E_F - E_{\text{VBM}}$  for the Si(111)( $\sqrt{3}\times\sqrt{3}$ )R 30°-B surface and K/Si(111) interfaces from the coverage dependence of the Si 2p core-level energy. However, this procedure is not completely straightforward because Si 2p core-level spectra are generally composed of a bulk component and one or more surface components.<sup>62</sup> In order to deduce the Fermi-level shift, the spectra must be decomposed into surface and bulk components and the adsorbate-induced shift of the bulk component must be determined. Unfortunately, the individual components cannot be clearly resolved, partially because of the limited instrumental resolution (0.5 eV at  $h\nu = 120$  eV). Therefore, we rely on a least-squares curve fitting of the experimental data. In order to decide whether our fits are physically meaningful, we not only relied on the residuals of our fits but also compared our results with published high-resolution Si 2p core-level studies.<sup>60,62</sup>

Usually,  $E_F - E_{\text{VBM}}$  for the clean Si(111) $7\times 7$  surface is taken as  $0.63 \pm 0.05$  eV.<sup>61</sup> It should, however, be realized that this value was an average over several samples, i.e.,



the Fermi-level position at the clean Si(111)7×7 surface may differ slightly from sample to sample. Therefore, we determined  $E_F - E_{\text{VBM}}$  independently by measuring the surface photovoltage (SPV) at 77 K.<sup>63,64</sup> In the following sections, we analyze our Si 2*p* core-level spectra in detail and determine the magnitude of the band bending.

#### A. The clean Si(111)7×7 surface

Si 2*p* core-level spectra of the clean Si(111)7×7 surface were collected at RT and at 77 K. In Fig. 11, we show the decomposition of the RT spectrum into a bulk component (*B*) and two surface components (*S*<sub>1</sub> and *S*<sub>2</sub>), riding on a smooth polynomial background. Each peak represents a Lorentzian spin-orbit doublet, convoluted with a Gaussian. Fitting parameters are listed in Table I. Our results are in excellent agreement with high-resolution studies.<sup>60,62</sup> The *S*<sub>2</sub> surface core level has been attributed to the rest atoms in the (7×7) reconstruction.<sup>62</sup> Since the rest-atom states are completely filled, the rest atoms accommodate excess negative charge, resulting in a core-level shift toward lower binding energy. The origin of the *S*<sub>1</sub> surface core level is less clear. It has been suggested that it originates from the adatoms and their nearest neighbors in the (7×7) reconstruction.<sup>62</sup> We will later show that these surface core levels are affected by the adsorption of K.

Upon cooling to 77 K, the spectrum has rigidly shifted to lower kinetic energy by 0.49 eV. This phenomenon is well known and can be attributed to a combination of a

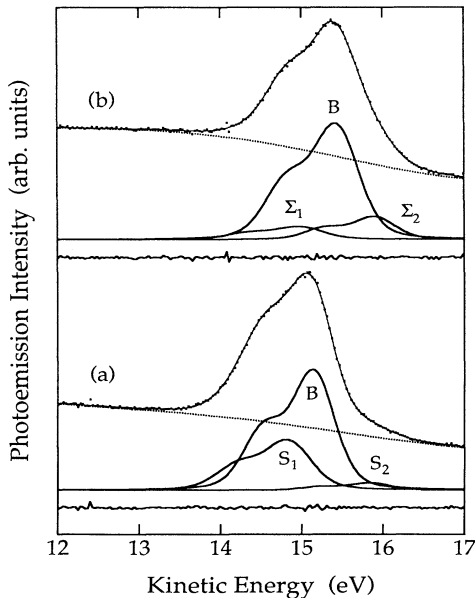


FIG. 11. Normal emission Si 2*p* core-level spectra for the clean Si(111)7×7 surface (a) and RT saturated K/Si(111)7×7 interface (b). The photon energy was 120 eV. The angle of incidence was 45°. The solid lines are the result of a least-squares fitting procedure, as explained in the text. The dotted lines represent a polynomial background function. Parameters are listed in Table I.

TABLE I. Fitting parameters for the Si 2*p* core-level spectra in Fig. 11. The following parameters were fixed: spin-orbit splitting (0.614 eV), branching ratio (0.5), Lorentzian full width at half maximum (FWHM) (0.150 eV), and Gaussian FWHM (0.51 eV for the bulk component and 0.55 eV for the surface components).

	Si(111)7×7	K/Si(111)7×7
Binding energy		
Si 2 <i>p</i> <sub>3/2</sub> (eV)		
<i>B</i>	99.79	99.51
<i>S</i> <sub>1</sub>	100.11	
<i>S</i> <sub>2</sub>	99.03	
$\Sigma$ <sub>1</sub>		99.96
$\Sigma$ <sub>2</sub>		99.06
Relative intensity		
$I_B/I_{\text{total}}$	0.67	0.70
$I_{S_1, \Sigma_1}/I_{\text{total}}$	0.29	0.12
$I_{S_2, \Sigma_2}/I_{\text{total}}$	0.04	0.18

surface photovoltage effect<sup>63,64</sup> and a temperature shift of  $E_F$ . For our wafers,  $E_{\text{CBM}} - E_F$  is 0.24 eV at RT and 0.04 eV at 77 K.<sup>65</sup> Hence, the temperature dependence of  $E_F$  accounts for a spectral shift of 0.20 eV toward low kinetic energy. Consequently, the SPV must account for the additional shift of 0.29 eV. It can easily be shown that the SPV generates flat-band conditions at 77 K, whereas it is negligible at RT.<sup>66</sup> Hence, the SPV shift at 77 K (0.29 eV) simply equals the band bending at RT. This implies that at RT, the Fermi level is located at 0.29 + 0.24 = 0.53 eV below the conduction-band minimum (CBM) or, equivalently, 0.59 eV above the VBM. The estimated margin of error is  $\approx 50$  meV. Note that our result is slightly different from Himpsel, Hollinger, and Pollak.<sup>61</sup> It is, however, very close to the SPV measurements by Demuth *et al.*<sup>63,67</sup>

#### B. The K/Si(111)7×7 interface

Upon K deposition, both the energy and line shape of the Si 2*p* core-level spectrum have changed [Fig. 11(b)]. Similar to the clean (7×7) surface, this spectrum can be fit with a single bulk component (*B*) and two surface components ( $\Sigma$ <sub>1</sub> and  $\Sigma$ <sub>2</sub>). The fitting parameters are listed in Table I. Magnusson *et al.* obtained qualitatively similar fits for the Cs/Si(111)7×7 interface.<sup>60</sup> The surface core-level shift for the  $\Sigma$ <sub>2</sub> component is 0.31 eV smaller than for the related *S*<sub>2</sub> component at the clean (7×7) surface. The relative intensity of the  $\Sigma$ <sub>2</sub> component is strongly enhanced. The total surface-to-bulk intensity ratios, however, are approximately the same for the clean Si(111)7×7 surface and K/Si(111)7×7 interface, suggesting that  $\Sigma$ <sub>2</sub> increased at the expense of  $\Sigma$ <sub>1</sub>. Intuitively, it might be thought that the low binding energy component ( $\Sigma$ <sub>2</sub>) should originate from the surface atoms, which are directly bonded to K atoms. However, the  $\Sigma$ <sub>2</sub> component is the main surface component, indicating that other surface atoms contribute to the  $\Sigma$ <sub>2</sub> component.

Very recently, Ma *et al.* published high-resolution Si  $2p$  core-level spectra of the K/Si(111) $7\times 7$  interface.<sup>29</sup> In their work, no attempt was made to fit the spectra. However, it was concluded that the  $S_2$  core level of the clean Si(111) $7\times 7$  surface shifts to higher binding energy upon K adsorption, which is at least qualitatively similar to our observation. They attributed this shift to a K-induced charge redistribution between the rest atoms and adatoms in the ( $7\times 7$ ) reconstruction. Although this interpretation might be quite plausible, we believe that this core-level shift simply indicates that the rest atoms are somehow involved in the interfacial bonding. At this stage, we consider any interpretation regarding the origin of the surface core levels at the K/Si(111) $7\times 7$  interface as highly speculative.

As mentioned before, the Si  $2p$  core-level spectrum of the Cs/Si(111) $7\times 7$  interface can also be decomposed into one bulk and two surface core levels. A major difference, however, is that the surface core levels of the Cs/Si(111) $7\times 7$  interface appear to be asymmetric. Magnusson *et al.* introduced a Doniach-Sunjić (DS) line shape<sup>68</sup> in order to fit the surface core levels, indicating that the Cs/Si(111) $7\times 7$  interface has become metallic at RT saturation coverage. In contrast, our spectra appear perfectly symmetric. Thus unlike the Cs/Si(111) $7\times 7$  interface, the K/Si(111) $7\times 7$  interface is nonmetallic, in agreement with the valence-band spectra.

From the K-induced energy shift of the bulk component ( $B$ ), we can determine the position of the Fermi level. Compared to the clean Si(111) $7\times 7$  surface the bulk component has shifted 0.28 eV toward high kinetic energy. Hence, at the RT saturated K/Si(111) $7\times 7$  interface,  $E_F - E_{\text{VBM}}$  equals  $0.59 - 0.28 = 0.31$  eV.

### C. The Si(111)( $\sqrt{3}\times\sqrt{3}$ )R 30°-B surface

The Si  $2p$  core-level spectrum of the clean Si(111)( $\sqrt{3}\times\sqrt{3}$ )R 30°-B surface is shown in Fig. 12. It is obvious that this spectrum must be composed of more than one spin-orbit doublet. According to McLean, Terminello, and Himpsel, the spectra of the clean surface can be fit with two spin-orbit doublets.<sup>69</sup> In their high-resolution study, they identified a bulk component and a surface component, shifted to high binding energy. This B-induced surface component was analyzed in more detail by Rowe, Wertheim, and Riffe.<sup>70</sup> In their study, it was argued that the surface component is composed of several unresolved contributions from inequivalent Si atoms in the first three layers near the surface. Our spectrum was fit with two Gaussian broadened spin-orbit-split Lorentzian doublets [Fig. 12(a)]. The fitting parameters are listed in Table II. The energy separation between the bulk component ( $B$ ) and surface component ( $\Gamma$ ) is 0.47 eV, which is slightly larger than the splitting reported by McLean, Terminello, and Himpsel (0.40 eV) but very close to the one reported by Rowe, Wertheim, and Riffe (0.48 eV). We therefore conclude that the fit of our unresolved core-level spectrum is reliable. From the binding energy of the bulk Si  $2p$  core level, we infer that  $E_F$  is located 0.11 eV above the VBM.

A comparison with other studies is quite interesting.

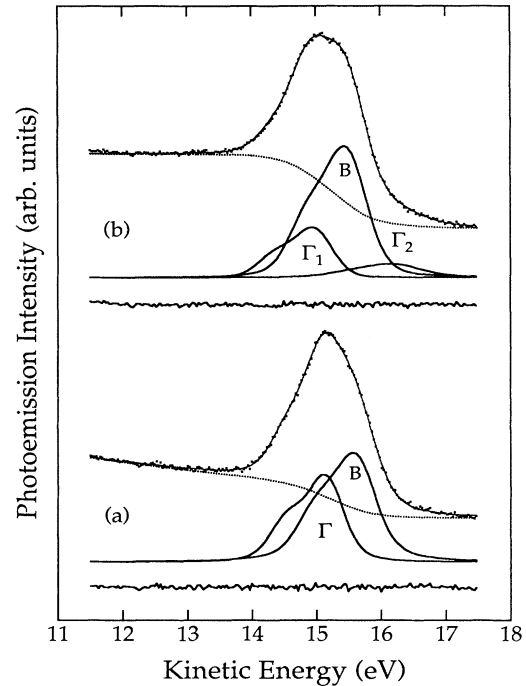


FIG. 12. Normal emission Si  $2p$  core-level spectra for the clean Si(111)( $\sqrt{3}\times\sqrt{3}$ )R 30°-B surface (a) and RT saturated K/Si(111)( $\sqrt{3}\times\sqrt{3}$ )R 30°-B interface (b). The photon energy was 120 eV. The angle of incident was 45°. The solid lines are the result of a least-squares fitting procedure, as explained in the text. The dotted lines represent an integrating background function. Parameters are listed in Table II.

In the core-level study by McLean, Terminello, and Himpsel,<sup>69</sup>  $E_F$  was located  $\sim 0.5$  eV above the VBM. In that study, the Si(111)( $\sqrt{3}\times\sqrt{3}$ )R 30°-B surface reconstruction was obtained after segregating B to the surface of very heavily B-doped Si(111) wafers ( $2\times 10^{19}$  cm $^{-3}$ ). Rowe, Wertheim, and Riffe<sup>70</sup> used even higher dopant levels ( $1.5\times 10^{20}$  cm $^{-3}$ ). In their study,  $E_F$  was located below the VBM, i.e., the surface is metallic, probably due to the degenerate dopant levels. Apparently,  $E_F$  critically depends on the B concentration near the surface. Hence, in order to interpret our result on  $n$ -type Si, we must consider the different preparation techniques and their implications for the band bending measurements in detail.

Previous studies on the heavily B-doped samples revealed an unusual high intensity for the surface-shifted component in the Si  $2p$  core-level spectrum. While our ratio surface-to-bulk intensity ratio was only 0.7 ( $E_{\text{kin}} = 14.5$  eV), McLean, Terminello, and Himpsel and Rowe, Wertheim, and Riffe reported 0.9 and 2.0, respectively. A surface-to-bulk intensity ratio of 0.7 suggests that the surface-shifted component arises solely from Si atoms directly bonded to the B atoms, and from the adatoms (see the Appendix). On the other hand, Rowe, Wertheim, and Riffe argued that their surface-to-bulk intensity ratio of 2.0 means that their surface stoichiometry

TABLE II. Fitting parameters for the Si  $2p$  core-level spectra in Fig. 12. The following parameters were fixed: spin-orbit splitting (0.614 eV), branching ratio (0.5), and Gaussian FWHM [0.55 eV for the Si(111)( $\sqrt{3}\times\sqrt{3}$ )R 30°-B surface and 0.62 eV for the K/Si(111)( $\sqrt{3}\times\sqrt{3}$ )R 30°-B interface]. In order to get a better fit, we allowed the Lorentzian FWHM to vary (Ref. 71).

	Si(111)( $\sqrt{3}\times\sqrt{3}$ )R 30°-B	K/Si(111)( $\sqrt{3}\times\sqrt{3}$ )R 30°-B
Binding energy		
Si $2p_{3/2}$ (eV)		
$B$	99.31	99.44
$\Gamma$	99.78	
$\Gamma_1$		99.94
$\Gamma_2$		98.68
Relative intensity		
$I_B/I_{\text{total}}$	0.59	0.68
$I_\Gamma/I_{\text{total}}$	0.41	
$I_{\Gamma_1}/I_{\text{total}}$		0.23
$I_{\Gamma_2}/I_{\text{total}}$		0.09
Lorentzian FWHM (meV)		
$B$	317	194
$\Gamma$	183	
$\Gamma_1$		82
$\Gamma_2$		462

must be nearly ideal, provided that second-neighbor atoms also contribute to the surface core-level signal. Following their analysis, it may seem that our surface must be B deficient. However, in that case one would expect to observe surface-state emission from the partially filled dangling-bond states of the Si adatoms, which pin the Fermi level at approximately 0.5 eV above the VBM.<sup>33,34,42,69</sup> Since we do not observe any surface states above the VBM, we can safely assume that our surface is not B deficient. In fact, it is very likely that surfaces prepared by B segregation have excess B in the near surface region.

Our measurements on  $n$ -type samples show that  $E_F$  is located in the lower part of the band gap, suggesting a large band bending of  $\approx 0.8$  eV. If our surface was perfectly stoichiometric and ordered, one would expect that the surface would be unpinned with  $E_F$  close to the CBM. The large upward band bending can only be understood if the Si(111)( $\sqrt{3}\times\sqrt{3}$ )R 30°-B surface has surface states or defects states close to VBM. Most likely, this is not the case. A reasonable conclusion is that the sample has become  $p$  type directly beneath the surface. This idea is corroborated by the fact that we did not observe a SPV shift at 77 K. If the sample has become  $p$  type with  $E_F - E_{\text{VBM}} = 0.1$  eV, flat-band conditions exist near the surface which readily explains the absence of a SPV effect. We conclude that excess B is present beneath the surface. Note that since the donor concentration is only  $3\times 10^{15}$  cm $^{-3}$  or 1 donor atom per  $1.67\times 10^7$  Si atoms, very tiny amounts of B diffusing into the bulk already compensate the donor atoms near the surface, resulting in a  $p$ -type selvedge.

#### D. The K/Si(111)( $\sqrt{3}\times\sqrt{3}$ )R 30°-B interface

The Si  $2p$  core-level spectrum of the Si(111)( $\sqrt{3}\times\sqrt{3}$ )R 30°-B surface changes dramatically upon K ad-

sorption [Fig. 12(b)]. Based on the high-resolution spectrum of this interface as reported by Ma *et al.*,<sup>30</sup> we fit our spectrum using a single bulk component and two surface-shifted components riding on an integrated background. There are a few unexpected observations. First, the energy splitting between the bulk component ( $B$ ) and the main surface component ( $\Gamma_1$ ) does not change upon K absorption. Second, the total surface-to-bulk intensity ratio decreases by about 30%. Third, the width of the surface component at low binding energy ( $\Gamma_2$ ) is much larger than for the other peaks.<sup>71</sup> The presence of  $\Gamma_2$  was considered evidence for substantial charge transfer.<sup>30</sup> Unfortunately, it is hard to compare our fit with the data by Ma *et al.*, because their surface-to-bulk intensity ratios

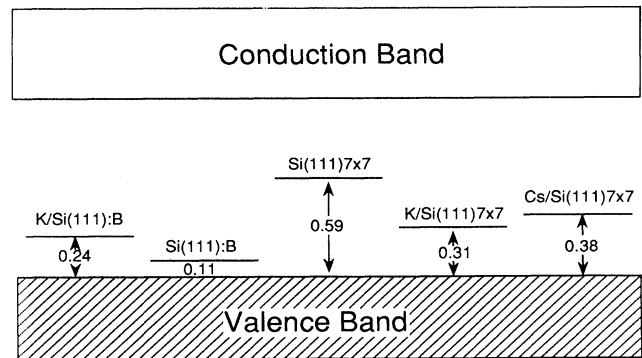


FIG. 13. Schematic diagram, showing the pinning positions (in eV) of the Fermi level at the clean Si(111)7 $\times$ 7 and Si(111)( $\sqrt{3}\times\sqrt{3}$ )R 30°-B surfaces and at the room-temperature saturated K/Si(111)7 $\times$ 7 and Cs/Si(111)( $\sqrt{3}\times\sqrt{3}$ )R 30°-B interfaces. The data for the Cs/Si(111)7 $\times$ 7 interface were taken from Magnusson *et al.* (Ref. 60). The estimated margins of error are  $\approx 50$  meV.

are very different, due to differences in sample preparation (B segregation) and surface sensitivity.

The bulk Si  $2p$  core level has shifted  $\approx 0.13$  eV toward low kinetic energy as compared to the clean Si(111)( $\sqrt{3}\times\sqrt{3}$ ) $R30^\circ$ -B surface, indicating downward band bending near the interface. Hence, the Fermi level at the K/Si(111)( $\sqrt{3}\times\sqrt{3}$ ) $R30^\circ$ -B interface is located 0.24 eV above the VBM. This is similar to the observation by Ma *et al.*, suggesting that the pinning position at this interface is intrinsic to the ( $\sqrt{3}\times\sqrt{3}$ ) surface structure and does not significantly depend on the preparation conditions. It is also close to the Fermi-level position at the K/Si(111)7 $\times$ 7 interface, suggesting a common pinning mechanism. In fact, in both cases,  $E_F$  might be pinned by the low-binding-energy tail of the K-induced surface states near the center of the SBZ. A similar pinning mechanism was proposed for the Cs/Si(111)7 $\times$ 7 interface.<sup>60</sup> The Fermi-level positions at the clean surfaces and K/Si(111) interfaces are summarized in a schematic diagram (Fig. 13).

### V. K $3p$ CORE-LEVEL SPECTRA AT ROOM TEMPERATURE

K  $3p$  core-level spectra were recorded as a function of coverage up to saturation. In Fig. 14, we show the K  $3p$  core-level spectra for the K/Si(111)7 $\times$ 7 interface (a) and K/Si(111)( $\sqrt{3}\times\sqrt{3}$ ) $R30^\circ$ -B interface (b). Coverage-dependent binding energies are plotted in Fig. 15. We first discuss the line shape of these core-level spectra. Binding energies will be discussed in Sec. V B.

#### A. Line-shape analysis

The linewidths of the K  $3p$  core-level spectra from the K/Si(111)7 $\times$ 7 and K/Si(111)( $\sqrt{3}\times\sqrt{3}$ ) $R30^\circ$ -B interfaces are much larger than one would expect on the basis of our experimental resolution ( $\approx 0.25$  eV). In fact, spectra from a thick K film, grown at low temperature, clearly reveal the spin-orbit-split components ( $\Delta_{s.o.} = 0.26$  eV; see also Refs. 72 and 73). Near saturation coverage, our spectra appear very broad and asymmetric. The large width of the core-level spectra seems to be a general property of alkali-metal adsorbates on metals and semiconductors<sup>73,74,77</sup> and has been attributed to vibrational broadening and to core-hole decay through an *interatomic* Auger process.<sup>73,75</sup> However, we must consider other mechanisms to account for the *asymmetric* broadening of the K  $3p$  spectra near saturation coverage. Usually, asymmetric broadening of core-level spectra is attributed to metallic screening of the core hole, resulting in a DS line shape.<sup>68</sup> However, this would be in severe conflict with our valence-band photoemission data and work function measurements. Furthermore, the surface components in the Si  $2p$  core-level spectra appear to be *symmetric*. In order to resolve this controversy, we have tried to fit the K  $3p$  photoemission from the saturated K/Si(111)7 $\times$ 7 interface using a Gaussian broadened DS function. As shown in Fig. 16(a), it is possible to roughly reproduce the asymmetric line shape. However, in order to do so, an unphysical background has to be assumed

(dotted line). Moreover, the residuals reveal that this fit is very unsatisfactory. In Fig. 16(b), we used two DS functions. The quality of the fit is much better, though still not satisfactory. A slight problem with this fit is that the intensity of the threshold peak becomes negative near the low-binding-energy cutoff which is, of course, unphysical. An even better fit is obtained by introducing three Gaussian-broadened Lorentzians [Fig. 16(c)]

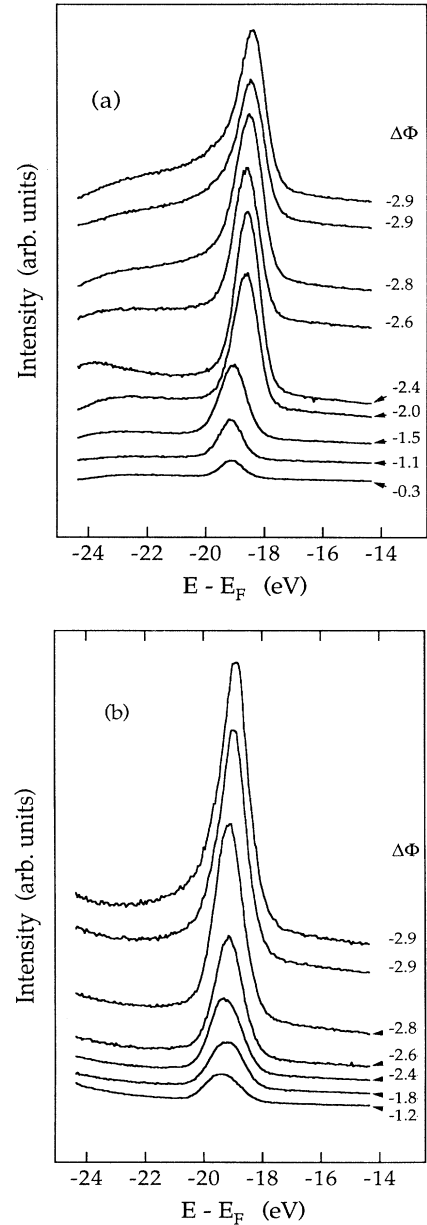


FIG. 14. Coverage dependence of the normal emission K  $3p$  core-level spectra of the K/Si(111)7 $\times$ 7 interface (a) and K/Si(111)( $\sqrt{3}\times\sqrt{3}$ ) $R30^\circ$ -B interface (b) at room temperature. The photon energy is 30.8 eV. The angle of incidence is  $45^\circ$ . The corresponding work function lowering is indicated at the right side of each spectrum.

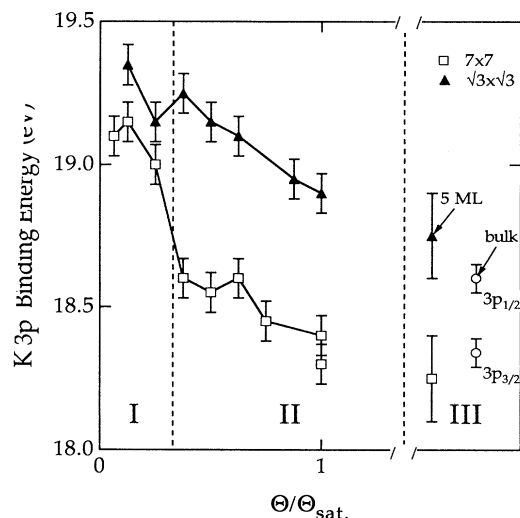


FIG. 15. Coverage dependence of the K 3p core-level binding energies for the K/Si(111)7 $\times$ 7 and K/Si(111)( $\sqrt{3}\times\sqrt{3}$ )R30 $^\circ$ -B interfaces. The data from regime III were recorded from a thick K film, grown at 77 K.

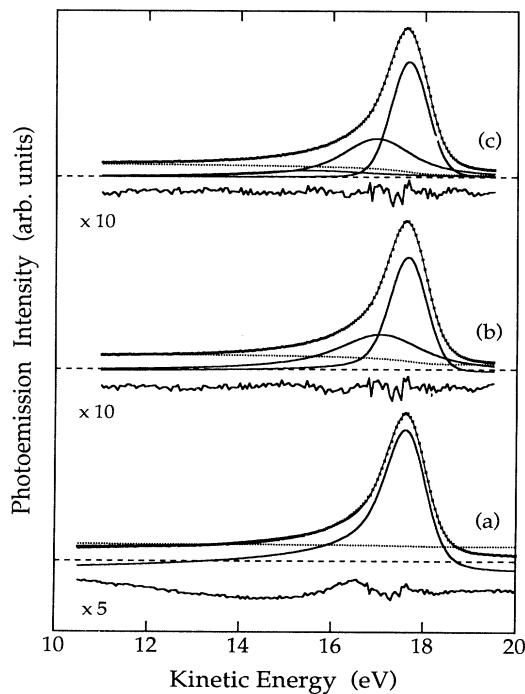


FIG. 16. Least-squares fits of the K 2p core-level spectrum from the room-temperature saturated K/Si(111)7 $\times$ 7 interface, using a single DS function in (a), two DS functions in (b), and three Lorentzians in (c). These line shapes were convoluted with a Gaussian (FWHM is 0.8 eV). The residuals of each fit are plotted, using scale factors as indicated. The dashed lines represent the zero level for each spectrum. The dotted lines represent an integrating background. The spectrum was recorded at normal emission, using a photon energy of 41.2 eV. The angle of incidence was 45 $^\circ$ .

without introducing asymmetry parameters. Of course, as the number of parameters is increased, a better fit can always be obtained. Therefore, we believe that a physical interpretation of the fitting parameters is nebulous. However, from these fits we do learn that the apparent asymmetry does not demand metallicity. Furthermore, from (b) and (c) we learn that the Lorentzian width of the second and third peak at high binding energy dramatically increases with distance from the threshold peak. Therefore, it is unlikely that these peaks originate from inequivalent K atoms (different chemisorption sites). In that case, the photoemission spectrum probably represents the envelope of a finite number of final states. The same is true for the 3p core-level spectrum of the saturated K/Si(111)( $\sqrt{3}\times\sqrt{3}$ )R30 $^\circ$ -B interface (Fig. 17). Interestingly, the K 3p core-level spectra from the K/Si(100)2 $\times$ 1 interface are quite different and can be fit with DS functions.<sup>7</sup> However, unlike the K/Si(111) interfaces, the RT saturated K/Si(100) interface is metallic.<sup>4,6-8,13</sup> Apparently, the lack of core-hole screening at nonmetallic K/Si(111) interfaces allows shakeup satellites in the photoelectron spectrum, resulting in an asymmetric line shape that can easily be confused with that of a fully screened final state (DS function).

It is interesting to note that a qualitatively similar evolution of the core-level line shapes has been observed for the Cs 4d and 5p spectra from the Cs/GaAs(110) interface,<sup>9,76</sup> Li 1s spectra from the Li/Be(0001) interface,<sup>77</sup> and K 3p spectra from the K/Be(0001) interface.<sup>78</sup> Ap-

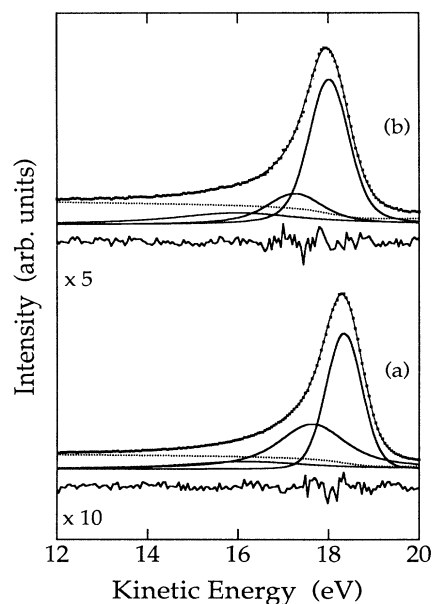


FIG. 17. Least-squares fits of the K 3p core-level spectrum for the RT saturated K/Si(111)7 $\times$ 7 (a) and K/Si(111)( $\sqrt{3}\times\sqrt{3}$ )R30 $^\circ$ -B (b) interfaces, using three Gaussian-broadened Lorentzians. The integrated background is indicated by a dotted line. The residuals are plotted, using scale factors as indicated. These spectra were recorded at normal emission, using a photon energy of 41.2 eV. The angle of incidence was 45 $^\circ$ .

parently, asymmetric broadening near saturation seems to be a rather general property of alkali-metal adsorbates. Of course, a definite interpretation of these phenomena requires a detailed evaluation of the dynamics of adsorbate core-hole screening. For some early theoretical work on this problem, we refer to the papers of Schönhammer and Gunnarsson.<sup>79</sup>

### B. K 3p core-level binding energies

The coverage dependence of the K 3p core-level binding energy is completely different for the K/Si(111)7×7 and K/Si(111)(√3×√3)R30°-B interfaces (Fig. 15). At the K/Si(111)(√3×√3)R30°-B interface, the binding energy decreases rather monotonically from 19.3 eV at low coverage to 18.8 eV at saturation. The 3p binding energy at the K/Si(111)7×7 interface decreases from 19.05 eV at low coverage to 18.25 eV at saturation, with a sudden drop below 0.5 ML. This sudden drop appears slightly beyond the metal-to-semiconductor transition. For comparison, the binding energies of the surface and bulk K 3p<sub>3/2</sub> core levels for bulk K are 18.54 and 18.34 eV, respectively.<sup>80</sup> We can roughly define three different coverage regimes, as indicated in Fig. 15. In regime I, the K/Si(111)7×7 interface is still metallic. In regime II, the K 3p core-level binding energy at the K/Si(111)7×7 interface is significantly reduced (≈0.5 to ≈0.7 eV) and the line shape becomes symmetric near RT saturation coverage. In this regime, the interface is nonmetallic. Finally, regime III corresponds to multilayer growth at low temperature, as discussed in Sec. VI.

A qualitative explanation of this behavior could be that K is present as an ionic species at low coverage. As the coverage increases, the K-Si bond weakens at the (7×7) interface whereas it remains strong and ionic at the (√3×√3) interface. This would be consistent with the conclusion of Ma *et al.*<sup>29,30</sup> However, this explanation is probably too naive since the Madelung potential at the core-hole site and the screening of the core hole should also be taken into account.<sup>81</sup>

It is interesting to note that the shift toward low binding energy also seems to be a rather general property of alkali metals and other electropositive adsorbates.<sup>73–77,81–84</sup> For instance, Riffe, Wertheim, and Citrin showed that the 3p core-level energy for K on W(110) decreases until the first layer is completed.<sup>73</sup> Nevertheless, it was concluded that the interfacial bonding is predominantly covalent over the entire coverage regime, even at very low coverage, suggesting that the binding energy shifts do not originate from the substrate-adsorbate interaction. Moreover, since the core-level binding energies behave qualitatively similar on the variety of substrates, it is likely that the reduction of the core-level binding energies with coverage has its origin mainly in the adsorbate-adsorbate interaction, mediated by the substrate at low coverage.<sup>82</sup> Furthermore, it must be realized that both the substrate-adsorbate coupling and adsorbate-adsorbate coupling changes upon photoionization.<sup>82</sup> This suggests that an explanation of the K 3p binding energies at the K/Si(111)7×7 and K/Si(111)(√3×√3)R30°-B interfaces in terms of initial-

state charge transfer may be too simplistic, even though we cannot rule out the possibility that the nature of the K-Si bond is different at these interfaces, as suggested by Ma *et al.*<sup>29,30</sup> We believe that core-level photoemission is inconclusive.

### VI. MULTILAYER GROWTH AT LOW TEMPERATURE

After preparation of the saturated K/Si(111)7×7 and K/Si(111)(√3×√3)R30°-B interfaces, the samples were cooled down to approximately 77 K to allow multilayer

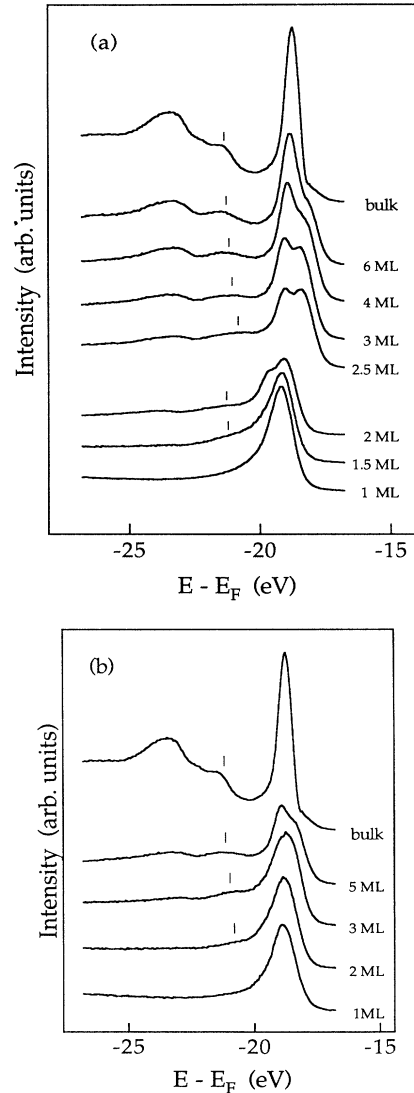


FIG. 18. K 3p core-level spectra ( $\alpha_i = 45^\circ$ ,  $\Theta_e = 0^\circ$ ) as a function of coverage for the K/Si(111)7×7 (a) and K/Si(111)(√3×√3)R30°-B interfaces. The spectra were recorded at 77 K. The photon energy was 41.2 eV. The plasmon-loss satellites are indicated by tick marks. The energy shift between 2 and 2.5 ML in (a) is due to a quenching of the surface photovoltage. The K/Si(111)(√3×√3)R30°-B interface does not exhibit a surface photovoltage (Sec. IV).

growth. Upon subsequent K deposition, the work function increases by about 0.5 eV, indicating that the interface has become metallic (Fig. 3).<sup>40</sup> Indeed, at  $\sim 2$  monolayers,<sup>85</sup> a clear Fermi edge can be observed (not shown). Moreover, at a coverage of  $\sim 1.5$  monolayers, a shakeup satellite appears in the K  $3p$  core-level spectra of both interfaces, as indicated by tick marks in Fig. 18. The energy separation between the threshold peak and this shakeup feature is roughly 2.0 eV at 1.5 ML and increases up to 2.7 eV for a very thick K film. The energy loss of 2.7 eV equals the surface plasmon energy of bulk K.<sup>86</sup> A similar coverage dependence of energy-loss features has been observed at other metal-semiconductor interfaces as well and is related to the development of free carrier interface plasmons.<sup>12,50,87</sup> This clearly indicates that the interface metallizes during the growth of a second K layer. A detailed high-resolution electron-energy-loss study of these plasmons will be published elsewhere.<sup>88</sup> We also observe another feature at a kinetic energy of roughly 23 eV. This feature is not due to shakeup processes but can simply be identified as the K  $M_{23}VV$  Auger peak.<sup>75</sup>

Finally, at a coverage of approximately 2.5 ML, we observe an abrupt quenching of the surface photovoltage effect at the K/Si(111) $7\times 7$  interface [Fig. 18(a)]. This phenomenon is related to long-range conductivity in the overlayer.<sup>89</sup> Interestingly, free carrier plasmon-loss features already appear in the spectrum before the surface photovoltage effect is quenched. We conclude that metallic screening (e.g., intraband plasmon excitation) takes place before the interface has become macroscopically conducting. Although the morphology of the subsequent layers is unknown, we speculate that the sudden onset of long-range conductivity is related to a percolation threshold of metallic K clusters on top of the first layer.

## VII. SUMMARY AND CONCLUSIONS

The adsorption of K onto the clean Si(111) $7\times 7$  and Si(111)( $\sqrt{3}\times\sqrt{3}$ ) $R30^\circ$ -B surfaces has been studied by angle-resolved photoemission spectroscopy, LEED, and work function measurements. At the RT saturated K/Si(111) $7\times 7$  and K/Si(111)( $\sqrt{3}\times\sqrt{3}$ ) $R30^\circ$ -B interfaces, a dispersionless K-induced surface state is present just below  $E_F$ . This state is responsible for the pinning of the Fermi level at  $\approx 0.25$  to  $\approx 0.3$  eV above the VBM.

At the K/Si(111)( $\sqrt{3}\times\sqrt{3}$ ) $R30^\circ$ -B interface, a second interface state is observed for  $\Theta_e > 20^\circ$ , at  $\approx 2.2$  eV below  $E_F$ . This state can readily be identified as the backbond surface state of the Si adatoms in the B-induced ( $\sqrt{3}\times\sqrt{3}$ ) surface reconstruction. The persistence of this state upon K adsorption indicates that the K atoms directly bond to the dangling bonds of the Si adatoms, leaving all Si-Si bonds intact. On this basis, we suggest that the absolute saturation coverage of this interface is  $\frac{1}{3}$  ML. The saturation coverage for the K/Si(111) $7\times 7$  interface is nearly equal.

On the basis of valence-band photoemission, Si  $2p$  core-level spectroscopy and work function measurements, we conclude that both interfaces are semiconducting at RT saturation coverage. Although the K  $3p$  core-level

spectra near saturation coverage appear to be asymmetric, our analysis reveals that this asymmetry does not demand metallic screening. Instead, the asymmetry is likely due to a finite number of shakeup excitations, due to the *lack of screening at these nonmetallic interfaces*.

The nonmetallic ground state of the K/Si(111)( $\sqrt{3}\times\sqrt{3}$ ) $R30^\circ$ -B interface cannot be understood on the basis of single-particle considerations and we argue that this interface represents a two-dimensional Mott insulator. The lower limit of the on-site Coulomb repulsion in the K-induced surface state is  $\approx 0.7$  eV. Although the semiconducting nature of the K/Si(111) $7\times 7$  interface can be understood in terms of a single-particle picture, we argue that the insulating nature of the interface at submonolayer coverages must also be due to electron correlation. More generally, we believe that these findings may have important implications for future theoretical studies of alkali-metal adsorption on semiconductors because so far, most studies have been based on single-particle electronic structure calculations.

Finally, we have shown that metallization occurs during the growth of a second K layer at low temperature. Evidence of metallization is based on the development of an intraband plasmon satellite in the K  $3p$  core-level spectrum above 1.5 ML and on the appearance of a Fermi edge in valence-band photoemission near 2 ML. The sudden quenching of the surface photovoltage effect at a coverage of approximately 2.5 ML marks the onset of long-range conductivity in the overlayer.

## ACKNOWLEDGMENTS

We thank Dr. P. F. Lyman for his assistance during the photoemission experiments at the NSLS and Professor L. Sneddon for providing purified decaborane. We also thank Professor R. P. Messmer for reading the manuscript critically. Financial support has been provided by the National Science Foundation, MRL program under Grant No. DMR91-20668 and by NSF-DMR91-20398.

## APPENDIX

The surface-to-bulk intensity ratio in the Si  $2p$  core-level spectrum of the Si(111)( $\sqrt{3}\times\sqrt{3}$ ) $R30^\circ$ -B can be calculated, using a "layer-by-layer attenuation" scheme. In this model, we assume that the core-level intensity from the outermost Si(111) double layer is directly proportional to the number of Si atoms within the double layer, including the adatoms. Furthermore, we assume that each double layer attenuates the core-level intensity from the double layer directly underneath by a factor  $\exp(-d/\lambda)$  where  $d$  is the average spacing between the Si double layers (3.1 Å) and  $\lambda$  the inelastic mean free path which depends on the kinetic energy of the photoelectrons. The number of Si atoms in a double layer is  $2N$ ,  $N$  being equal to the number of atoms in the (111) plane of Si. Based on the structural model for the Si(111)( $\sqrt{3}\times\sqrt{3}$ ) $R30^\circ$ -B surface (Fig. 1), we come to the following conclusions. The number of Si adatoms is equal to the number of B atoms and is exactly  $(\frac{1}{3})N$ . In the outermost double layer, the

number of Si atoms bonded directly to the subsurface B atoms is  $N$ . In this double layer, there are also  $(\frac{2}{3})N$  second-nearest-neighbor atoms (excluding the adatoms). In the second double layer,  $\frac{1}{3}N$  Si atoms are bonded directly to the B atoms. Furthermore, there are exactly  $N$  second-nearest-neighbor atoms in this double layer. If we assume that the Si  $2p$  surface core-level signal arises from the Si adatoms and form the Si atoms directly bonded to the B atoms, the surface-to-bulk intensity ratio  $R$  will be given by

$$R = \frac{\frac{4}{3} + \frac{1}{3} \exp(-d/\lambda)}{\frac{2}{3} + \frac{5}{3} \exp(-d/\lambda) + 2 \sum_{n=2}^{\infty} \exp(-nd/\lambda)}. \quad (\text{A1})$$

Likewise, if the second-nearest-neighbor atoms also contribute to the surface core-level signal, we obtain

$$R = \frac{2 + \frac{4}{3} \exp(-d/\lambda)}{\frac{2}{3} \exp(-d/\lambda) + 2 \sum_{n=2}^{\infty} \exp(-nd/\lambda)}. \quad (\text{A2})$$

It is easy to derive that

$$\sum_{n=2}^{\infty} \exp(-nd/\lambda) = \frac{\exp(-2d/\lambda)}{1 - \exp(-d/\lambda)}. \quad (\text{A3})$$

Therefore,  $R$  can be calculated exactly, provided that the inelastic mean free path  $\lambda$  is known. In our experiment, the kinetic energy of the photoelectron  $\approx 15$  eV. In that case, a typical value for  $\lambda \approx 4$  Å.<sup>69,70</sup> Using Eq. (A1), we then obtain  $R = 0.67$  which is very close to the experimental value. Alternatively, from Eq. (A2), we obtain  $R = 2.42$ . This strongly suggests that only the adatoms and the Si atoms bonded directly to the subsurface B atoms contribute to the Si  $2p$  surface core-level signal.

\*Present address: Department of Physics, University of Tennessee, Knoxville, TN 37996.

<sup>1</sup>K. H. Taylor and I. Langmuir, Phys. Rev. **44**, 224 (1933).

<sup>2</sup>See, e.g., H. Tochiwara, Surf. Sci. **126**, 523 (1983); T. Abukawa and S. Kono, Phys. Rev. B **37**, 9097 (1988); Y. Ling, A. J. Freeman, and B. Dely, *ibid.* **39**, 10144 (1989); I. P. Batra, *ibid.* **43**, 12322 (1991); Y. Morikawa, K. Kobayashi, K. Terakura, and S. Blügel, *ibid.* **44**, 3459 (1991).

<sup>3</sup>Y. Enta, S. Suzuki, S. Kono, and T. Sakamoto, Phys. Rev. B **39**, 5524 (1989); T. Abukawa, T. Kashiwakura, T. Okane, Y. Sasaki, H. Takahashi, Y. Enta, S. Suzuki, S. Kono, S. Sato, T. Kinoshita, A. Kakizaki, T. Ishii, C. Y. Park, S. W. Yu, K. Sakamoto, and T. Sakamoto, Surf. Sci. **261**, 217 (1992).

<sup>4</sup>L. S. O. Johansson and B. Reihl, Phys. Rev. Lett. **67**, 2191 (1991).

<sup>5</sup>P. Soukiassian, J. A. Kubby, P. Mangat, Z. Hurych, and K. M. Schirm, Phys. Rev. B **46**, 13471 (1992).

<sup>6</sup>U. A. Effner, D. Badt, J. Binder, T. Bertrams, A. Brodde, Ch. Lunau, H. Neddermeyer, and M. Hanbücken, Surf. Sci. **277**, 207 (1992).

<sup>7</sup>D. M. Riffe, G. K. Wertheim, J. E. Rowe, and P. H. Citrin, Phys. Rev. B **45**, 3532 (1992).

<sup>8</sup>S. Arekat, S. D. Kevan, and G. L. Richmond, Europhys. Lett. **22**, 377 (1993).

<sup>9</sup>T. Kendelewicz, P. Soukiassian, M. H. Bakshi, Z. Hurych, I. Lindau, and W. E. Spicer, Phys. Rev. B **38**, 7568 (1988).

<sup>10</sup>R. Cao, K. Miyano, T. Kendelewicz, I. Lindau, and W. E. Spicer, J. Vac. Sci. Technol. B **7**, 919 (1989).

<sup>11</sup>T. Maeda-Wong, D. Heskett, N. J. DiNardo, and E. W. Plummer, Surf. Sci. **208**, L1 (1989).

<sup>12</sup>N. J. DiNardo, T. Maeda Wong, and E. W. Plummer, Phys. Rev. Lett. **65**, 2177 (1990).

<sup>13</sup>E. G. Michel, P. Pervan, G. R. Castro, R. Miranda, and K. Wandelt, Phys. Rev. B **45**, 11811 (1992).

<sup>14</sup>L. J. Whitman, J. A. Stroschio, R. A. Dragoset, and R. J. Celotta, Science **251**, 1206 (1991).

<sup>15</sup>See, e.g., S. Ciraci and I. P. Batra, Phys. Rev. Lett. **56**, 877 (1986); **58**, 1982 (1987); Phys. Rev. B **37**, 8432 (1988).

<sup>16</sup>Y. Ling, A. J. Freeman, and B. Dely (Ref. 2).

<sup>17</sup>H. Ishida and K. Terakura, Phys. Rev. B **40**, 11519 (1989); R. V. Kasowski and M.-H. Tsai, Phys. Rev. Lett. **60**, 546 (1988).

<sup>18</sup>J. E. Klepeis and W. A. Harrison, J. Vac. Sci. Technol. B **7**, 964 (1989).

<sup>19</sup>R. M. Feenstra, J. Vac. Sci. Technol. B **7**, 925 (1989).

<sup>20</sup>O. Pankratov and M. Scheffler, Phys. Rev. Lett. **70**, 351 (1993).

<sup>21</sup>G. A. Allan and M. Lanoo, Surf. Sci. **63**, 11 (1977).

<sup>22</sup>J. E. Northrup, J. Ihm, and M. L. Cohen, Phys. Rev. Lett. **47**, 1910 (1981).

<sup>23</sup>W. A. Harrison, Phys. Rev. B **31**, 2121 (1985).

<sup>24</sup>C. B. Duke and W. K. Ford, Surf. Sci. **111**, L685 (1981).

<sup>25</sup>L. J. Whitman, J. A. Stroschio, R. A. Dragoset, and R. J. Celotta, Phys. Rev. B **44**, 5951 (1991).

<sup>26</sup>See, e.g., Y. Enta *et al.* (Ref. 3); S. Kono, K. Higashiyama, T. Kinoshita, T. Miyahara, H. Kato, H. Ohsawa, Y. Enta, F. Maeda, and Y. Yaegashi, Phys. Rev. Lett. **58**, 1555 (1987); L. S. O. Johansson, E. Landemark, C. J. Karlsson, and R. I. G. Uhrberg, *ibid.* **63**, 2092 (1989).

<sup>27</sup>If there is an even number of valence electrons per unit cell, the interface will be metallic if two or more different interface states cross  $E_F$ .

<sup>28</sup>N. F. Mott, *Metal-Insulator Transitions*, 1st ed. (Taylor and Francis, London, 1974).

<sup>29</sup>Y. Ma, C. T. Chen, G. Meigs, F. Setts, G. Illing, and H. Shigakawa, Phys. Rev. B **45**, 5961 (1992).

<sup>30</sup>Y. Ma, J. E. Rowe, E. E. Chaban, C. T. Chen, R. L. Headrick, G. M. Meigs, S. Modesti, and F. Sette, Phys. Rev. Lett. **65**, 2173 (1990).

<sup>31</sup>R. J. Hamers, R. M. Tromp, and J. E. Demuth, Phys. Rev. Lett. **56**, 1972 (1986).

<sup>32</sup>U. Backes and H. Ibach, Solid State Commun. **40**, 575 (1981).

<sup>33</sup>I.-W. Lyo, E. Kaxiras, and Ph. Avouris, Phys. Rev. Lett. **63**, 1261 (1989).

<sup>34</sup>E. Kaxiras, K. C. Pandey, F. J. Himpsel, and R. M. Tromp, Phys. Rev. B **41**, 1262 (1990).

<sup>35</sup>P. Bedrossian, R. D. Maede, K. Mortensen, D. M. Chen, J. A. Golovchenko, and D. Vanderbilt, Phys. Rev. Lett. **63**, 1257 (1989).

<sup>36</sup>R. L. Headrick, I. K. Robinson, E. Vlieg, and L. C. Feldman, Phys. Rev. Lett. **63**, 1253 (1989).

<sup>37</sup>A. Ishizaki and Y. Shiraki, J. Electrochem. Soc. **133**, 666 (1986).

<sup>38</sup>G. V. Hansson and R. I. G. Uhrberg, Surf. Sci. Rep. **9**, 197 (1988).

<sup>39</sup>At the Si(111)7×7 surface, the "metallic" surface state  $S_1$  is dispersionless and located  $\approx 0.2$  eV below  $E_F$ . In contrast,



- real metals are characterized by a dispersive energy band, crossing the Fermi energy at  $k = k_F$ . Hence, the photoemission experiment does not provide real evidence for a metallic ground state of the Si(111)7×7 surface. On the other hand, scanning tunneling microscopy (Ref. 31) and EELS (Ref. 32) data indicate that the Si(111)7×7 surface is truly metallic.
- <sup>40</sup>D. Heskett, T. Maeda Wong, A. J. Smith, W. R. Graham, N. J. DiNardo, and E. W. Plummer, *J. Vac. Sci. Technol. B* **7**, 915 (1989).
- <sup>41</sup>K. O. Magnusson and B. Reihl, *Phys. Rev. B* **41**, 12071 (1990).
- <sup>42</sup>T. M. Grehk, P. Mårtensson, and J. M. Nicholls, *Phys. Rev. B* **46**, 2357 (1992).
- <sup>43</sup>R. I. G. Uhrberg, G. V. Hansson, J. M. Nicholls, P. E. S. Persson, and S. A. Flodström, *Phys. Rev. B* **31**, 3805 (1985).
- <sup>44</sup>T. Kinoshita, S. Kono, and T. Sagawa, *Phys. Rev. B* **32**, 2714 (1985).
- <sup>45</sup>T. Kinoshita, S. Kono, and T. Sagawa, *Solid State Commun.* **56**, 681 (1985).
- <sup>46</sup>J. M. Nicholls, P. Mårtensson, G. V. Hansson, and J. E. Northrup, *Phys. Rev. B* **32**, 1333 (1985).
- <sup>47</sup>J. E. Northrup, *Phys. Rev. Lett.* **57**, 154 (1986); **53**, 683 (1984).
- <sup>48</sup>E. W. Plummer and W. Eberhardt, *Adv. Chem Phys.* **49**, 533 (1982).
- <sup>49</sup>I. Ivanov, A. Mazur, and J. Pollman, *Surf. Sci.* **92**, 365 (1980).
- <sup>50</sup>P. Soukiassian, M. H. Bakshi, Z. Hurych, and T. M. Gentle, *Surf. Sci.* **221**, L759 (1989).
- <sup>51</sup>W. Beall Fowler and R. J. Elliott, *Phys. Rev. B* **34**, 5525 (1986).
- <sup>52</sup>J. Stuke, *Philos. Mag.* **B 52**, 25 (1985).
- <sup>53</sup>N. M. Johnson, W. B. Jackson, and M. D. Moyer, *Phys. Rev. B* **31**, 1194 (1985).
- <sup>54</sup>R. J. Hamers and J. Demuth, *Phys. Rev. Lett.* **60**, 2527 (1988).
- <sup>55</sup>In a simple two-dimensional tight-binding model, including nearest-neighbor interactions only, the bandwidth  $W$  of the eigenvalue spectrum is given by  $W = 8t$ , where  $t$  represents the nearest-neighbor hopping integral.
- <sup>56</sup>D. Jeon, T. Hashizume, T. Sakurai, and R. F. Willis, *Phys. Rev. Lett.* **69**, 1419 (1992).
- <sup>57</sup>The intensity ratios of the K-*LMM* and Si-*L<sub>23</sub>VV* Auger signals were determined in a separate experiment. At RT saturation coverage,  $I_K/I_{Si}$  is 0.36 and 0.32 for the (7×7) and ( $\sqrt{3} \times \sqrt{3}$ ) interfaces, respectively. This indicates that the absolute coverages of these interfaces are indeed very close.
- <sup>58</sup>If the dangling bonds at the corner holes of the (7×7) reconstruction are also taken into account, the absolute saturation coverage becomes  $19/49 = 0.39$  ML.
- <sup>59</sup>P. Mårtensson, W.-X. Ni, G. V. Hansson, J. M. Nicholls, and B. Reihl, *Phys. Rev. B* **36**, 5974 (1987).
- <sup>60</sup>K. O. Magnusson, S. Wiklund, R. Dudde, and B. Reihl, *Phys. Rev. B* **44**, 5657 (1991).
- <sup>61</sup>At the clean Si(111)7×7 surface,  $E_F - E_{VBM} = 0.63$  eV, as determined by F. J. Himpsel, G. Hollinger, and R. A. Pollak, *Phys. Rev. B* **28**, 7014 (1983).
- <sup>62</sup>C. J. Karlsson, E. Landemark, L. S. O. Johansson, U. O. Karlsson, and R. I. G. Uhrberg, *Phys. Rev. B* **41**, 1521 (1990).
- <sup>63</sup>J. E. Demuth, W. J. Thompson, N. J. DiNardo, and R. Imbihl, *Phys. Rev. Lett.* **56**, 1408 (1986).
- <sup>64</sup>M. Alonso, R. Cimino, and K. Horn, *Phys. Rev. Lett.* **64**, 1947 (1990).
- <sup>65</sup>S. M. Sze, *Physics of Semiconductor Devices*, 2nd ed. (Wiley, New York, 1981).
- <sup>66</sup>Since the dopant level of our Si wafer is low, we can neglect tunneling as a mechanism for carrier recombination. Hence, the photocurrent is balanced only by recombination through thermionic emission. Using thermionic emission theory, it can easily be shown that the thermionic emission current exceeds the photocurrent at RT whereas it is negligible at 77 K [see, e.g., M. H. Hecht, *J. Vac. Sci. Technol. B* **8**, 1018 (1990)].
- <sup>67</sup>In Ref. 63, different dopant levels were used. From the SPV shift in that study, we obtain  $E_F - E_{VBM} = 0.61 \pm 0.05$  eV.
- <sup>68</sup>S. Doniach and M. Šunjić, *J. Phys. C* **3**, 285 (1970).
- <sup>69</sup>A. B. McLean, L. J. Terminello, and F. J. Himpsel, *Phys. Rev. B* **41**, 7694 (1990).
- <sup>70</sup>J. E. Rowe, G. K. Wertheim, and D. M. Riffe, *J. Vac. Sci. Technol. A* **9**, 1020 (1991).
- <sup>71</sup>In order to obtain a fit with nearly random residuals, we allowed the Lorentzian full width at half maximum to be different for each component. Although a satisfactory explanation is lacking, it is likely that this parameter is affected by background subtraction and/or inhomogeneity.
- <sup>72</sup>D. M. Riffe, G. K. Wertheim, D. N. E. Buchanan, and P. H. Citrin, *Phys. Rev. B* **45**, 6216 (1992).
- <sup>73</sup>D. M. Riffe, G. K. Wertheim, and P. H. Citrin, *Phys. Rev. Lett.* **64**, 571 (1990).
- <sup>74</sup>M. Domke, T. Mandel, C. Laubschat, M. Preitsch, and G. Kaindl, *Surf. Sci.* **189/190**, 268 (1987).
- <sup>75</sup>Up to RT saturation coverage, the K *M<sub>23</sub>VV* Auger intensity was below our detection limit. A plausible explanation is that the decay of the 4s electron into the 3p photohole is suppressed if a substantial fraction of the K valence charge is donated to the substrate [see, e.g. D Heskett, I. Strathy, E. W. Plummer, and R. A. de Paola, *Phys. Rev. B* **32**, 6222 (1985)].
- <sup>76</sup>T. Maeda Wong, N. J. DiNardo, D. Heskett, and E. W. Plummer, *Phys. Rev. B* **41**, 12342 (1990).
- <sup>77</sup>P. A. Brühweiler, G. M. Watson, and E. W. Plummer, *Surf. Sci.* **269/270**, 653 (1992).
- <sup>78</sup>B. S. Itchkawitz (unpublished).
- <sup>79</sup>K. Schönhammer and O. Gunnarsson, *Solid State Commun.* **23**, 691 (1977); **26**, 399 (1978).
- <sup>80</sup>B. S. Itchkawitz, Ph.D. thesis, University of Pennsylvania, 1991.
- <sup>81</sup>P. A. Schultz and R. P. Messmer, *Surf. Sci.* **209**, 229 (1989).
- <sup>82</sup>A. Stenborg, O. Björneholm, A. Nilsson, N. Mårtensson, J. N. Andersen, and C. Wigren, *Surf. Sci.* **211/212**, 470 (1989).
- <sup>83</sup>G. Pirug, A. Winkler, and H. P. Bonzel, *Surf. Sci.* **163**, 153 (1985).
- <sup>84</sup>J. J. Weimer and E. Umbach, *Phys. Rev. B* **30**, 4863 (1984).
- <sup>85</sup>The coverage at low temperature was estimated on the basis of deposition time, assuming sticking coefficients of 0.7 at RT and 1 at 77 K. The sticking coefficient at RT was estimated by comparing the work function decrease as a function of deposition time at RT and 77 K.
- <sup>86</sup>K. D. Tsuei, E. W. Plummer, and P. J. Feibelman, *Phys. Rev. Lett.* **63**, 2256 (1989).
- <sup>87</sup>S. Å Lindgren and L. Walldén, *Phys. Rev. B* **22**, 5976 (1980).
- <sup>88</sup>J. Chen, H. H. Weitering, N. J. DiNardo, and E. W. Plummer (unpublished).
- <sup>89</sup>G. D. Waddill, T. Komeda, Y.-N. Yang, and J. H. Weaver, *Phys. Rev. B* **41**, 10283 (1990).